

Stix et al. 1988
ER ID # 49680

10

Restoration of Compositional Zonation in the Bandelier Silicic Magma Chamber Between Two Caldera-Forming Eruptions: Geochemistry and Origin of the Cerro Toledo Rhyolite, Jemez Mountains, New Mexico

JOHN STIX,¹ FRASER GOFF,² MICHAEL P. GORTON,¹ GRANT HEIKEN,² AND SAMMY R. GARCIA³

The Cerro Toledo Rhyolite is a group of high-silica rhyolite domes and tephra that range in age from 1.45 to 1.12 Ma. The unit crops out in the Jemez Mountains of northern New Mexico and lies stratigraphically between the compositionally zoned upper and lower members of the Bandelier Tuff. The Cerro Toledo Rhyolite provides an exceptional opportunity to study the origin of compositional zonation in silicic magma chambers because it allows us to follow the restoration of the zonation with time between these two large caldera-forming ignimbrite eruptions. Based upon stratigraphic, geochronologic, and geochemical evidence, we have correlated different Cerro Toledo Rhyolite tephra units with groups of domes. Early Cerro Toledo Rhyolite domes appear to be located generally along the Toledo caldera ring fracture, whereas younger domes tend to cluster in the Toledo embayment. The Cerro Toledo Rhyolite appears to have tapped the most fractionated liquids at or near the top of the Bandelier magma chamber and records the restoration of compositional gradients over a period of 0.33 m.y. after the Lower Bandelier ignimbrite eruption. Cl, Rb, Cs, heavy rare earth elements, Y, Nb, Th, and U increase in concentration in progressively younger Cerro Toledo Rhyolite rocks. Because of depletions in K/Cs, Sr, Zr, Nb, and La/Yb over the same interval, we favor crystal fractionation of essentially quartz, alkali feldspar, zircon, and a light rare earth element enriched phase (probably allanite) as the primary mechanism by which the compositional gradients were reestablished. We believe diffusive processes did not play an important role because (1) certain cations of widely different valencies and diffusivities are not fractionated with respect to each other and (2) the observed chemical gradients conflict with those predicted by recent experimental Soret studies.

INTRODUCTION

The Cerro Toledo Rhyolite is a group of metaluminous high-silica rhyolite domes and associated tephra that crop out in and around the Toledo and Valles calderas in the Jemez Mountains of northern New Mexico. The Toledo and Valles calderas were formed at 1.45 and 1.12 Ma, respectively [Doell et al., 1968; Smith and Bailey, 1968; Smith et al., 1970] (Figure 1). The Cerro Toledo Rhyolite consists of silicic lava domes and tephra of fallout and surge origin. The unit is situated stratigraphically between the lower and upper members of the Bandelier Tuff (LBT and UBT, respectively) and is dated at 1.47-1.20 Ma [Izett et al., 1981; Heiken et al., 1986].

In contrast to the LBT and UBT, which are large-volume (250-400 km³) rhyolitic ignimbrites that were erupted geologically instantaneously during caldera collapse and are compositionally zoned, the Cerro Toledo Rhyolite is a product of explosive and effusive intracaldera activity that lasted 0.27-0.33 m.y. during the period between the two cataclysmic Bandelier eruptions. The Cerro Toledo Rhyolite thus occupies the interval between the caldera-forming events and records the restoration of chemical gradients and zonation within the Bandelier magma chamber [Smith, 1979]. The Cerro Toledo Rhyolite deposits may represent the products of the most fractionated liquids that collected at the top of the magma

chamber. Because the stratigraphy and age of the Cerro Toledo Rhyolite tephra and domes are well known [Izett et al., 1981; Goff et al., 1984; Heiken et al., 1986], we believe these rocks provide a window through which we are able to study the reestablishment of compositional zonation in a silicic magma chamber after a caldera-forming eruption. Ignimbrites only represent snapshots of compositional gradients in a magma chamber at an instant in time; in contrast, the Cerro Toledo Rhyolite allows us to follow the establishment of the gradients over 0.3 m.y., thus providing an opportunity to place much tighter constraints on the mechanisms involved.

It is the purpose of this study to (1) correlate Cerro Toledo Rhyolite domes and tephra by means of stratigraphy, geochemistry, and geochronology, (2) document and discuss geochemical variation of the Cerro Toledo Rhyolite, and (3) discuss the petrogenesis of the Cerro Toledo Rhyolite and the evolution of compositional zonation within the Bandelier magma chamber.

GEOCHRONOLOGY, GEOLOGY, AND MINERALOGY

Toledo domes and tephra are formally named the Cerro Toledo Rhyolite and lie stratigraphically between the LBT (Otowi Member), which was erupted at 1.45 Ma during formation of the Toledo caldera, and the UBT (Tshirege Member), erupted at 1.12 Ma from Valles caldera [Izett et al., 1981] (dates recalculated from Doell et al. [1968]). The locations of the Toledo and Valles calderas appear to be nearly coincident [Goff et al., 1984], and both may have formed by asymmetric trapdoor collapse with caldera fill thickening to the east [Nielson and Hulen, 1984; Heiken et al., 1986; Self et al., 1986]. The Cerro Toledo Rhyolite domes were first recognized by Griggs [1964] and mapped by Smith et al. [1970]. The Cerro Toledo Rhyolite tuffs were noted by Bailey et al. [1969] and also mapped by Smith et al. [1970], Izett et al. [1981] and Heiken

¹Department of Geology, University of Toronto, Canada.
²Earth and Space Sciences Division, Los Alamos National Laboratory, Los Alamos, New Mexico.
³Isotope and Nuclear Chemistry Division, Los Alamos National Laboratory, Los Alamos, New Mexico

Copyright 1988 by the American Geophysical Union

Paper number 7B7047
0148-0227/88/007B-7047\$05.00

Received by EPR-RPF
SEP 14 1995
Die



14006

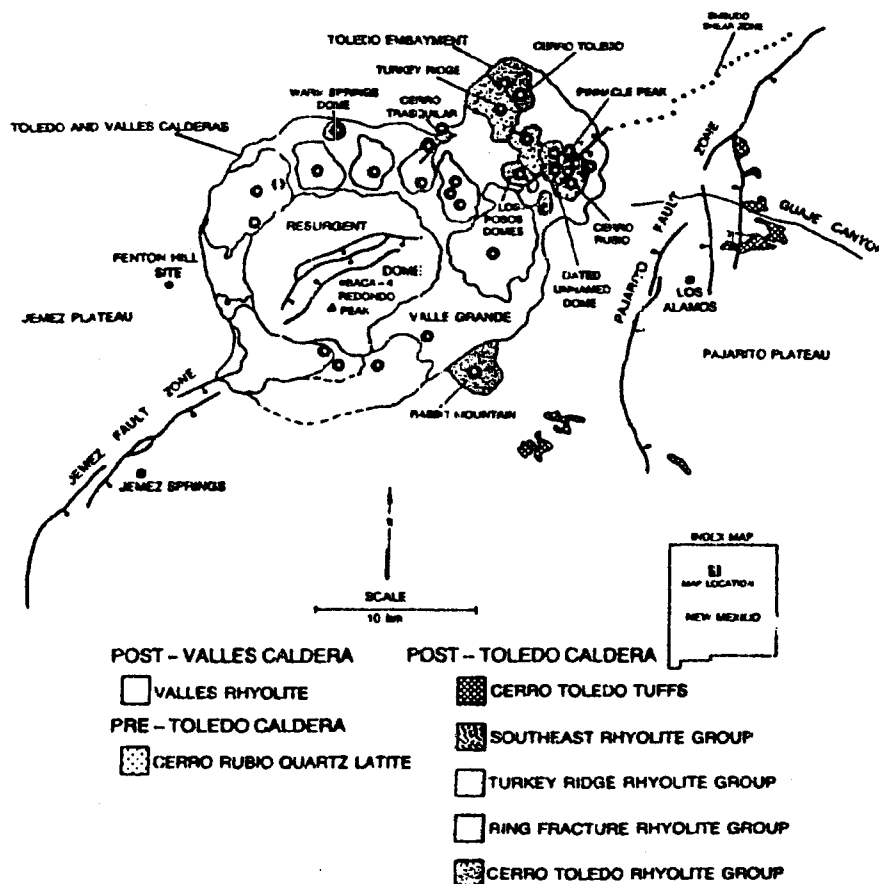


Fig. 1. Map showing the locations of Toledo and Valles calderas and Toledo embayment, Jemez Mountains, New Mexico. Cerro Toledo Rhyolite domes and lavas are shown by the stippled patterns; Cerro Toledo Rhyolite tephra are represented by the cross-hatched pattern. Locations of vents are indicated by the enclosed stars.

et al. [1986] have studied the stratigraphy, volcanology, and geochronology of the Cerro Toledo Rhyolite tephra in detail.

Domes

Cerro Toledo Rhyolite domes are conveniently divided into three groups: (1) A group of four domes, exposed within the north-northeast part of Valles caldera, forms a semicircular outcrop pattern, and is dated at 1.50–1.25 Ma [Heiken *et al.*, 1986] (Figure 1 and Table 1). These domes may represent remnants of ring fracture volcanism; in Toledo caldera [Goff *et al.*, 1984; Self *et al.*, 1986] and are referred to herein as the Toledo Ring Fracture (TRF) Group. (2) The second set of domes crops out in the Toledo embayment and consists of the Cerro Toledo (CT) Group, 1.50–1.33 Ma; the Southeast Rhyolite (SR) Group, 1.20 Ma; and the Turkey Ridge (TR) Group, 1.24 Ma (Figure 1 and Table 1). (3) The third locality is Rabbit Mountain (1.47 Ma), a dome and pyroclastics situated on the southeast margin of Valles caldera (Figure 1 and Table 1). Rabbit Mountain petrographically and geochemically resembles domes of the CT and has a similar K-Ar age.

Cerro Rubio quartz latite domes also crop out in the Toledo embayment (Figure 1). These domes are considerably older (2.2–3.6 Ma) than those of the Cerro Toledo Rhyolite (Table 1). The Cerro Rubio domes appear to be part of the Tschicoma Formation, a unit which consists of intermediate-composition lavas and pyroclastics that were erupted at 3.6–6.7 Ma [Loeffler, 1984]. These rocks may represent parental magmas of the Cerro Toledo Rhyolite and Bandelier Tuff.

Our ongoing studies have so far shown that Cerro Toledo Rhyolite domes are composed primarily of glass (>90%), with lesser amounts of plagioclase (7–15%), hornblende ($\leq 5\%$), sanidine and quartz ($\leq 2\%$), biotite (<1%), and trace amounts of anorthoclase and hypersthene [Heiken *et al.*, 1986].

Tephra

Cerro Toledo Rhyolite tephra consists of Plinian pumice falls, fine-grained phreatomagmatic ash beds of fallout and surge origin that contain accretionary lapilli and epiclastic sedimentary rocks. Individual tephra units sometimes show

as also crop out in the
 domes are considerably
 the Cerro Toledo Rhyolite
 appear to be part of the
 it consists of intermediates
 that were erupted at 3.6-
 as may represent parental
 the said Bandelier Tuff.
 shown that Cerro Toledo
 arily of glass (> 90%) with
 13% hornblende (5.5%),
 tite (< 1%), and trace
 pyrite [Heiken et al.,

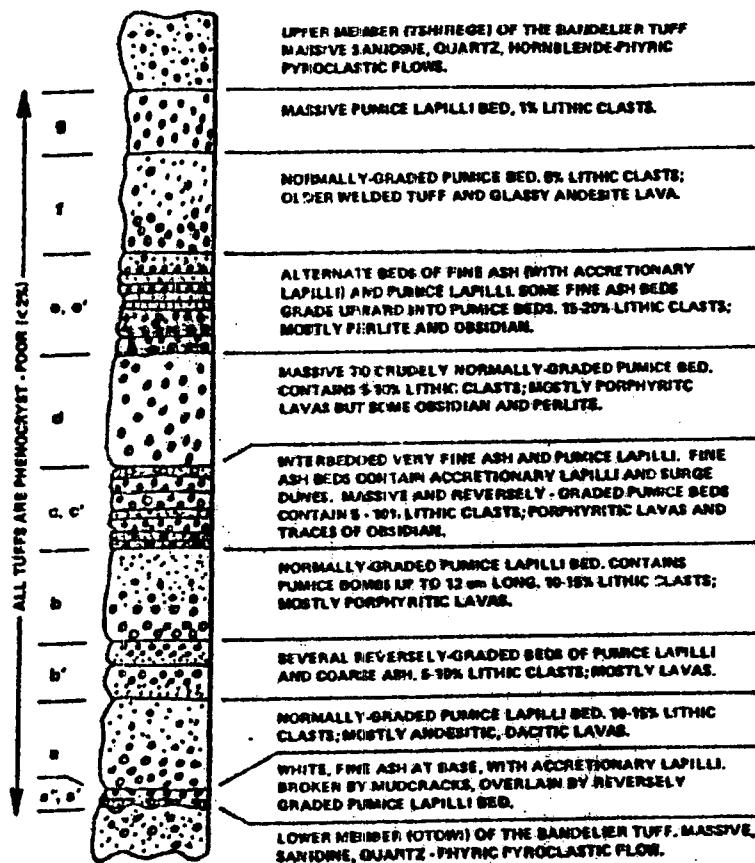
TABLE I Compilation of Potassium-Argon Dates From Tewa Group Rhyolites and Related Rocks in the Valles Caldera, Toledo Embayment, and Pajarito Plateau, Jemez Mountains, New Mexico

Sample*	Unit	Rock Type	Material	K, %	Radiogenic ⁴⁰ Ar, 10 ⁻¹¹ mol/g	Radiogenic ⁴⁰ Ar, %	Age,† 10 ⁶ years	Source‡	Comment
	Upper Member, Bandelier Tuff						1.12 ± 0.03	I	weighted mean of three age determinations
	Tsankawi Pumice	pumice	sanidine						
	Cerro Toledo Rhyolite								
	Pyroclastic units								
JS-6-5	Fall unit D?	pumice	sanidine	6.02	12.8	56.8	1.23 ± 0.02	I	mean of two fission-track ages isochron age from sanidine, plagioclase, and hornblende
	Fall unit C	pumice	glass + sanidine	3.928	5.590	13.3	1.52 ± 0.04	S	
	Fall unit B	pumice	zircon				1.43 ± 0.11	I	
		pumice					1.47 ± 0.04	I	
	Cerro Toledo Rhyolite								
	Toledo Embayment domes								
F81-150	Pinnacle Peak	obsidian	glass	3.74	7.797	46.3	1.20 ± 0.02	T	mean of two age determinations
PC-81-13	Turkey Ridge	rhyolite	sanidine	5.881	12.6	40.9	1.24 ± 0.03	Dr	mean of two age determinations
F81-148	Unnamed dome	obsidian	glass	3.71	8.382	20.0	1.33 ± 0.02	T	
F84-6	Rabbit Mountain	obsidian	glass + sanidine	3.682	9.135	45.6	1.43 ± 0.04	S	mean of two age determinations
F84-6	Rabbit Mountain	obsidian	glass	3.733	9.838	65.0	1.52 ± 0.06	Dr	
F84-9	Cerro Toledo	rhyolite	glass + sanidine	3.870	9.236	30.2	1.38 ± 0.05	S	
F81-146	Cerro Toledo	obsidian	glass	3.69	10.378	50.5	1.62 ± 0.02	T	
	Toledo Caldera moat domes								
	Warm Springs dome	rhyolite	sanidine	5.85	12.65	53.9	1.25 ± 0.04	Do	weighted mean of two age determinations
F81-139	Cerro Trasquilar	obsidian	glass	3.75	8.235	51.0	1.27 ± 0.03	T	mean of two age determinations
F84-12	East Los Posos dome	rhyolite	glass + sanidine	2.537	6.46	41.0	1.47 ± 0.05	S	mean of two age determinations
F83-27	West Los Posos dome	rhyolite	sanidine	5.595	14.6	45.0	1.50 ± 0.05	Dr	
	Lower Member, Bandelier Tuff						1.45 ± 0.06	I	weighted mean of three age determinations
	Guaje Pumice	pumice	sanidine						
614-84-8	Cerro Rubio Quartz Latite	dacite	plagioclase	0.428	1.618	44.1	2.18 ± 0.09	S	mean of two age determinations
F83-245	Dome north of Cerro Rubio	dacite	plagioclase	0.353	2.20	26.4	3.59 ± 0.36	Dr	
	Pre-Bandelier Ignimbrite								
F84-10	Ignimbrite B	pumice	sanidine	4.379	21.6	67.8	2.84 ± 0.07	S	mean of two age determinations
V81-56B	Ignimbrite A	pumice	sanidine	4.60	29.06	4	3.64 ± 1.64	K	

*JS-6-5 collected by J. Stix. PC-81-13 collected by P. Carrol; 614-84-8 collected by G. Valentine; V81-56B collected by S. Self; all F samples collected by F. Goff.
 †Here, $\lambda_1 = 0.58 \times 10^{-10} \text{ yr}^{-1}$, $\lambda_2 = 4.962 \times 10^{-10} \text{ yr}^{-1}$, $^{40}\text{K}/\text{K} = 1.167 \times 10^{-4}$; method of reporting error varies from lab to lab
 ‡Do, Dnell et al. [1968]; Dr, R. Drake, University of California, Berkeley; I, Izett et al. [1981]; K, D. Krummenacher, San Diego State University; S, M. Shafigullah, University of Arizona; T, S. Tamanyu, Geological Survey of Japan. Many dates have been previously reported by Goff et al. [1984]; Heiken et al. [1986], and Self et al. [1986].

STIX ET AL.: RESTORATION OF COMPOSITIONAL ZONATION

10 - 000000 - 0000



COMPOSITE STRATIGRAPHIC SECTION, CERRO TOLEDO TUFFS.

Fig. 2. Composite stratigraphic column, Cerro Toledo Rhyolite tephra. The tephra consist of pumice falls and phreatomagmatic ash, as well as reworked volcanoclastic debris. Units c and e show rapid fluctuations between pumice falls and fine-grained phreatomagmatic deposits (c', e'). No scale is indicated because of the variable thickness of the tephra at different localities. Where they crop out, the tephra range from less than 1 m to 22 m thick.

gradation from phreatomagmatic ash at the base into coarsest pumice falls upward (Heiken et al., 1986). The tephra is found in a 20-km-wide band to the east of the Toledo embayment centered near Los Alamos and in a 4-km-wide blanket from Rabbit Mountain to the southeast of Valles caldera (Heiken et al., 1986) (Figure 1). A possible subsurface intracaldera facies of Cerro Toledo Rhyolite tephra is represented by the S_3 sandstone of Nielson and Hulen [1984] in the vicinity of the resurgent block of Valles caldera. The S_3 sandstone thickens eastward to 70 m at a depth of 1709 m in borehole B-4.

The stratigraphy of the Cerro Toledo Rhyolite tephra near Los Alamos is summarized below from Heiken et al. [1986]. The tephra consists of seven major units (Figure 2), beginning with units a, a', and a'' at the base, which consist of pumice falls having some fine ash with mud cracks. Above, units b and b' are Plinian fallout beds. Unit b is dated at 1.47 ± 0.04 Ma [Izett et al., 1981] (Table 1). Unit c consists of fine tuff

with accretionary lapilli (c') and pumice falls (c) and has an age of 1.52 ± 0.04 Ma. Unit d is dated at 1.23 ± 0.02 Ma [Izett et al., 1981]. Unit d is a pumice fall, whereas unit e contains fine ash with accretionary lapilli (e') alternating with pumice beds (e). Typically, fine ash grades upward into pumice lapilli and coarse ash. Unit e is similar to c. Units f and g are both pumice falls.

Cerro Toledo Rhyolite tephra is composed predominantly of glass (>95%). Sandstone does not exceed 5% and quartz 1%, whereas the Bandelier Tuff contains 5-20% sandstone and 5-15% quartz [Smith and Bailey, 1966; Heiken et al., 1986]. We have so far identified the following minor phases in Cerro Toledo Rhyolite tephra: plagioclase, augite, hypersthene, hornblende, biotite, Fe-Ti oxides, and traces of zircon and allanite [Heiken et al., 1986]. These minerals do not exceed 1%. For example, unit b contains only 0.00014 wt % zircon [Izett et al., 1981].

CORRELATION BETWEEN CERRO TOLEDO
RHYOLITE DOMES AND TEPHRA

Geochemical Methods

Major elements were analyzed by X ray fluorescence (XRF) at Los Alamos following the procedures of Valentine [1983], except for samples 14-2, 14-4, 14-5, 14-7, 14-8, 15-1, and 15-2, which were analyzed by electron microprobe [Heiken et al., 1986]. Rb, Sr, Y, Zr, and Nb were run by XRF at Toronto following Norrish and Chappell [1977]. Cl, Cs, Co, Sc, rare earth elements (REE), Hf, Ta, Th, and U were analyzed by instrumental neutron activation analysis (INAA) methods at Los Alamos after Garcia et al. [1982] and Minor et al. [1982]. Table 2 gives accuracy and precision for replicate analyses of NIM-G. Table 3 lists pertinent geochemical data for individual samples.

Correlations

Figure 3 shows a composite chemostratigraphy of Cerro Toledo Rhyolite tephra assembled from individual samples of five stratigraphic sections through the tuffs. We previously have correlated individual tephra units among sections by means of marker beds (e.g., units c and e) and geochemistry, as detailed by Heiken et al. [1986]. We discuss the correlations between domes and tephra generally in order of decreasing age and refer the reader to Figure 3 and Tables 1, 3, and 4.

Older Cerro Toledo Rhyolites

Tephra units a-a' are relatively depleted in Rb and Nb, for example, compared with the younger parts of the stratigraphy. These units do not appear to correlate with any Cerro Toledo Rhyolite domes. The oldest domes may have been obliterated or buried during subsequent explosive activity of the Cerro Toledo Rhyolite and UBT. The Los Posos domes (1.50-1.47 Ma, TRF) correlate well with tephra units b and b' (1.47 Ma) with respect to age and chemistry. For example, elements such as Rb (domes 139-145 ppm, tuffs 139-145 ppm) and Sr (domes 20-23 ppm, tuffs 21-24 ppm) bear strong resemblance. However, Zr shows somewhat poorer agreement (domes 162-168 ppm, tuffs 134-144 ppm). This may be a result of variable crystal contents between tephra and domes and/or changing zircon saturation levels between the time of tephra eruptions and emplacement of the domes, due to different amounts of water and/or different temperatures of the tephra and dome magmas [Harrison and Watson, 1983; Watson and Harrison, 1983, 1984].

Rabbit Mountain (average date 1.47 Ma) and Cerro Toledo (average 1.50 Ma, CT) have similar ages to that of units b and b'. The domes are enriched in Nb, Rb, and Y and depleted in Sr compared with the tuffs (Table 3), suggesting either that the eruptions were compositionally zoned or that the domes were not the source of the tephra units.

Middle Cerro Toledo Rhyolites

The Turkey Ridge domes (1.24 Ma, TR) appear intermediate geochemically between older TRF domes (1.50-1.47 Ma, Los Posos) and younger TRF domes (1.27-1.25 Ma, Warm Springs dome, Cerro Trasquilar). Elements such as Nb, Rb, and heavy rare earth elements (HREE) clearly display this trend (e.g., TR 85-89 ppm Nb, TRF 69-150 ppm Nb). The Turkey Ridge domes may represent the source of tephra in and/or between units d and e. This would be consistent with respect to age, because unit d is dated at 1.23 Ma [Izett et al.,

TABLE 2. Precision and Accuracy for Trace Element Analyses of NIM-G by XRF and INAA

Element	n	x, ppm	1σ, ppm	Accepted Values, ppm	
				Abbey [1983]	Gorvandaraju [1984]
Cl	13	270	40	170*	170*
Rb	8	319	2	320	320
Cs	13	1.2	0.5	1*	1*
Sr	8	12.1	0.2	10	10
La	13	123	7	105*	109
Ce	13	222	16	200	195
Nd	13	69	10	68*	72
Sm	13	16	2	16*	15.8
Eu	13	0.5	0.3	0.4*	0.35
Dy	13	20	2	15*	17*
Yb	13	157	0.7	14	14.2
Lu	13	2.1	0.2	2*	2*
Y	8	137.7	0.7	145	143
Zr	8	291	1	300	300
Hf	13	13.4	0.6	12*	12*
Nb	8	54.7	0.9	53	53
Th	13	52	3	52	51
U	13	17.4	0.1	15*	15*

1981]. However, K/Cs ratios of the domes ($7.7-8.4 \times 10^3$) favor a correlation in units c and/or d (K/Cs $8.0-8.4 \times 10^3$). One possible problem is that these domes carry phenocrysts, whereas the tuffs are nearly aphyric. An exact geochemical correlation is not possible in this case as with units b and b'; however, the data do suggest that the sources of units d and/or c were the Turkey Ridge domes.

Younger Cerro Toledo Rhyolites

With respect to Nb, Rb, Y, Th, and U, the Southeast Rhyolite dome (1.20 Ma, SR) and welded tuffs of Pinnacle Peak show close correspondence with unit e. Heiken et al. [1986] have suggested that a tuff ring in which the welded tuff is found was the source of unit e. Because unit e is less than 1.23 Ma [Izett et al., 1981], the geochronology is consistent between dome and tephra. Three objections to this correlation are (1) the dome carries phenocrysts, whereas the tuffs are practically aphyric, (2) the dome has very low Sr, whereas unit e has 6 ppm Sr, (3) the REE content of the domes does not match that of unit e, and (4) the K/Cs ratios of the domes ($4.3-4.7 \times 10^3$) are lower than those of unit e (K/Cs $5.8-6.8 \times 10^3$). The second problem is a general one between Cerro Toledo Rhyolite domes and tephra, the third may be an analytical effect, and the fourth suggests the domes lie stratigraphically between unit f and the Tsankawi Pumice (K/Cs $5.2-2.8 \times 10^3$).

Warm Springs dome (1.25 Ma, TRF) and Cerro Trasquilar (1.27 Ma, TRF) are also possible sources of units e-g. Certain trace elements such as Rb, Nb, Zr, Y, and U show close agreement. However, Cerro Trasquilar also is depleted in Sr with respect to the tuffs. The K/Cs ratios of the domes ($3.7-4.6 \times 10^3$) again indicate that the domes are situated between unit f and the Tsankawi Pumice (Table 3).

Tsankawi Pumice Bed of UBT

The Tsankawi Pumice bed represents the initial Plinian deposit from the eruption that formed Valles caldera at 1.12 Ma [Doell et al., 1968]. The Tsankawi thus overlies and postdates the Cerro Toledo Rhyolite. It is therefore interesting that Warm Springs dome (1.25 Ma, TRF) has trace element con-

ITS:

f.

NE
E
DS
ND

f:

f
f

C

LL

ESIVE,

f pumice falls and
ns between pumice
kness of the tephraumice falls (c) and has an
dated at 1.23 ± 0.02 Ma
mice fall, whereas unit e
lapilli (e') alternating with
rades upward into pumice
lar to c. Units f and g arecomposed predominantly
t exceed 5% and quartz
ains 5-20% sanidine and
66; Heiken et al., 1986].
ng minor phases in Cerro
se, augite, hypersthene,
nd traces of zircon and
minerals do not exceed
nly 0.00014 wt % zircon

TABLE 3a. Geochemical Analysis

Number*	Unit									
	a'	a'	a'	a	b'	b'	b'	b	b	c
SiO ₂	...	78.1	78.0	78.1
TiO ₂	...	0.16	0.04	0.10
Al ₂ O ₃	12.1	12.2	12.1	11.6	11.9	12.1	11.3	11.9	11.9	11.4
Fe ₂ O ₃	1.71	1.06	1.01	1.18	1.08	0.82	1.08	0.93	...	0.89
MnO	0.06	0.05	0.07	0.06	0.06	0.07	0.06	0.06	0.06	0.06
MgO	...	0.02	0.04	0.04
CaO	0.48	0.32	0.32	0.43	...	0.37	0.51	0.39	0.47	0.34
Na ₂ O	3.80	3.24	3.74	3.48	3.60	3.57	3.69	3.75	3.69	3.56
K ₂ O	4.94	4.58	4.66	4.32	4.58	4.87	4.77	4.54	5.08	4.18
P ₂ O ₅
LOI
Total	...	99.73	99.98	100.04
Cl	700	900	1000	900	1300	1300	1700	1100	1100	1200
Rb	99	132	140	...	145	139	138	139
Cs	2.8	2.4	3.0	3.8	3.8	1.7	4.1	3.9	4.2	4.3
Sr	30	8.1	7	...	21	23	24	25
La	72	50	49	50	4	43	41	44	40	42
Ce	149	107	95	126	43	86	104	87	97	88
Nd	...	31	33	28
Sm	8.6	6.5	7.8	6.8	7.5	5.9	6.2	7.4	6.4	6.4
Eu	0.34	0.20	0.12	0.23	0.22	0.18	0.29	0.20	0.29	0.24
Dy	5.7	6.7	6.9	6.6	6.8	6.5	6.8	6.4	5.9	6.2
Yb	3.7	4.3	4.4	4.4	4.5	4.5	4.0	4.1	4.4	3.9
Lu	0.64	0.67	0.69	0.72	0.67	0.70	0.70	0.63	0.67	0.68
Y	36	43	42	...	44	42	42	42
Zr	309	161	140	...	144	133	136	134
Hf	9.6	6.0	5.4	6.4	5.2	5.5	6.2	4.9	5.3	6.0
Nb	50	63	65	...	67	64	62	63
Th	14	17	17	17	17	18	17	18	17	17
U	4.3	5.1	5.5	5.6	6.0	5.8	6.0	5.7	5.7	5.7

Analyzed samples are combined pumice lapilli that were handpicked and cleaned ultrasonically prior to being crushed.

*Tephra samples were collected from four stratigraphic sections, indicated by the prefix in the sample number. The four sections are located on the Guaje Mountain 2 1/2-min quadrangle, section 6, NW 1/4, T19N, R6E, sec 13; section 14, SW 1/4, T19N, R6E, sec 10; section 15; SW 1/4, T19N, R6E, sec 11; section 25, SW 1/4, T20N, R6E, sec 14.

tents remarkably similar to the basal Tsankawi Pumice (sample 6-8) that is exposed above Cerro Toledo Rhyolite tephra in the eastern Jemez Mountains (e.g., Warm Springs dome 298 ppm Rb, Tsankawi 297 ppm Rb). However, light rare earth elements (LREE) do not agree so well between these two units. Furthermore, K-Ar ages conflict, and *Self et al.* [1986] have placed the source of the Tsankawi near Redondo Peak from isopach data (Figure 1). Sample 6-8 may not represent the true base of the Tsankawi Pumice because it is not enriched in Rb, for example, compared with other samples of Tsankawi collected in the Jemez Mountains (J. Wolff, University of Texas, unpublished data, 1987). Indeed, the thickness of Tsankawi Pumice is much less to the east of Valles caldera than to the west [*Self et al.*, 1986]. Although sample 6-8 and Warm Springs dome seemingly correlate with respect to geochemistry (but not age), sample 6-8 may represent a less evolved part of the Tsankawi Pumice, erupted at 1.12 Ma, and may correspond to a certain level of compositional zonation in the Bandelier magma chamber that was also tapped by the eruption of Warm Springs dome at 1.25 Ma. This level of zonation may have been situated at a greater depth in the magma chamber at 1.12 Ma than at 1.25 Ma.

Discussion

Clearly, Cerro Toledo Rhyolite domes are the source of Cerro Toledo Rhyolite tephra and were associated with explosive volcanic activity. The eruptions appear to be a result of high water content of the magma [*Newhall and Melson,*

1983]. Certain tephra units are in part phreatomagmatic (e.g., units c' and c') (Figure 2). *Heiken et al.* [1986] suggested the tuffs erupted through a lake in the topographically low north-eastern part of Valles caldera and Toledo embayment.

Because of refinements in our knowledge of Toledo caldera and Toledo embayment, the Cerro Toledo Rhyolite tephra are not merely a sequence of tuffs from most rhyolite eruptions. The above age and geochemical correlations suggest that the location of source domes for Cerro Toledo Rhyolite tephra changed, in part, from ring fracture domes in Toledo caldera in early Cerro Toledo Rhyolite time to Toledo embayment domes in middle to late Cerro Toledo Rhyolite time. The locus of explosive volcanism then changed dramatically to near Redondo Peak at 1.12 Ma during eruption of UBT [*Self et al.*, 1986]. The structural emplacement of domes in Toledo embayment is probably not coincidental because the Jemez fault zone, resurgent dome faults, Toledo embayment, and Santa Clara shear zone define the trace of the Jemez lineament, a zone of crustal weakness intermittently active from Precambrian to Quaternary time [*Aldrich, 1986*].

GEOCHEMICAL VARIATION WITHIN THE CERRO TOLEDO RHYOLITE

Domes

Younger TRF domes (Warm Springs, Cerro Trasquilar, 1.27-1.25 Ma) are depleted in LREE, Eu, and Sr and are

Geochemical Analyses

Unit	
c	e
6-4	6-5
...	...
11.8	11.4
0.89	0.89
0.06	0.06
...	...
0.34	0.48
3.69	3.56
4.18	4.36
...	...
...	...
1200	1000
139	153
4.3	4.3
25	15
42	32
88	82
...	...
6.4	6.1
0.24	0.23
6.2	7.2
3.9	5.0
0.68	0.72
47	47
134	135
6.0	5.9
63	69
17	18
5.7	6.1

of Cerro Toledo Rhyolite Tephra

c	c	d	d?	e	e	e	e	e	e	f
14.4	15.3	6.6	15.11	6.7	15.1	15.7	15.12	15.2	25.1	15.6
77.9	77.8	77.7
0.11	0.02	0.06
12.0	11.2	12.1	11.6	11.6	12.2	11.6	11.7	12.2	11.3	12.1
0.99	1.04	1.10	1.07	1.12	1.11	1.18	1.16	1.00	1.12	1.19
0.03	0.05	0.06	0.07	0.07	0.06	0.07	0.07	0.11	0.07	0.08
0.4	0.43	0.04	0.02
0.37	0.51	0.45	...	0.26	0.26	...	0.28	0.25	0.66	...
3.38	3.03	3.86	3.90	3.88	3.59	3.63	3.76	3.50	2.56	3.77
5.19	4.78	4.99	4.52	4.98	4.61	4.95	5.13	5.14	5.04	4.36
...
100.01	99.69	99.98
900	1000	1600	1500	1600	1400	1700	1700	1100	1800	1700
...	...	159	190	197	...	200	197	202
...	4.2	4.9	6.0	6.1	6.2	6.3	7.3	5.5	5.1	6.9
...	...	23	30	5.7	...	3.1	5.0	4.4
45	38	43	41	33	33	33	35	36	38	38
101	78	98	79	80	75	86	80	81	79	78
28	29	24	26	27	...
6.4	7.2	7.4	7.5	8.1	6.6	7.9	7.8	5.9	7.1	8.4
0.21	0.14	0.30	0.18	0.22	...	0.08	0.21	0.12	0.12	0.18
5.4	6.7	7.9	9.2	8.9	9.2	9.4	9.3	9.6	9.3	11
4.2	4.7	4.6	6.5	6.0	6.5	6.1	7.2	5.8	6.2	7.6
0.68	0.71	0.79	0.99	1.0	0.96	1.1	1.1	0.86	0.96	1.0
...	...	50	64	66	...	66	67	69
...	...	150	157	161	...	161	163	168
6.0	5.8	5.9	7.0	7.1	7.5	7.3	8.4	6.9	6.9	7.0
...	...	77	91	95	...	95	94	96
18	18	19	21	22	22	22	23	20	20	22
5.5	5.8	6.9	8.1	8.1	8.0	8.0	8.0	6.9	6.9	8.2

Four sections are located at sections 15; SW 1/4, T19N,

matic (e.g., [1986]) suggested the geographically low north-embayment, edge of Toledo caldera. Rhyolite tephra are from rhyolite eruptions. Relations suggest that the Toledo Rhyolite tephra times in Toledo caldera to Toledo embayment to Rhyolite time. The changed dramatically to eruption of UBT [Self et al. 1986] because the Jemez lineament active from ca. 1986].

WITHIN THE UBT

at Cerro Trasquilar, Eu, and Sr and are

enriched in HREE, Y, Cs, Rb, Nb, Th, and U compared with the older TRF domes (Los Posos, 1.5-1.47 Ma). In contrast, CT and SR domes exhibit comparatively little chemical variation with age for many elements (e.g., Rb, Zr, Nb, Th, U), although some variability exists for REE, Y, and Cs. TR domes show generally lower concentrations of Rb, Zr, Hf, Nb, Y, and U compared with CT and SR domes (Table 3).

The above relationships suggest that the chemical compositions of Cerro Toledo Rhyolite domes are, in part, structurally controlled by the location of Toledo caldera. Intracaldera ring fracture domes (TRF) show large geochemical changes with time and thus may be connected to the main Bandelier magma chamber. Extracaldera domes (CT, SR) exhibit much more limited temporal chemical evolution and may be eruptive products of a series of smaller, isolated magma bodies in which geochemical processes operated similarly but did not enrich or deplete different elements so efficiently. As an example, Rabbit Mountain (CT) crops out on the southeast margin of Toledo caldera and is isolated from the other domes of Toledo embayment (Figure 1); however, Rabbit Mountain has many geochemical similarities to other CT and SR domes. The lower concentrations of Rb, Zr, Hf, Nb, Y, and U within TR domes, compared with CT and SR domes, may reflect a small, isolated magma chamber that evolved somewhat differently from those of CT and SR domes. Because the Jemez lineament probably controlled the ascent of magma, the TR domes may have been supplied with different amounts of magma at differing rates and times compared with the CT and SR domes.

Tephra

The relative ages of the different Cerro Toledo Rhyolite tephra units are well understood because of good time-stratigraphic control. Due to stratigraphic juxtaposition, we are able to examine temporal geochemical relationships between the LBT and UBT and the Cerro Toledo Rhyolite tephra. The tephra sequence shows systematic geochemical variations with time more clearly than do the Cerro Toledo Rhyolite domes.

Many trace elements vary systematically in concentration upsection through the Cerro Toledo Rhyolite stratigraphic column (Figures 3 and 4). Cl, Ca, Rb, Nb, Y, Th, U, and HREE are enriched upward. For example, Nb increases upward from 50 ppm at the base of the Cerro Toledo Rhyolite to 156 ppm at the Tsankawi Pumice bed. In contrast, LREE decrease irregularly in concentration upsection through most of the sequence but increase at unit e and above. Zr decreases to a minimum in the middle of the sequence, then increases upward from there. However, the Zr/Nb ratio decreases upsection. Likewise, the K/Ca and [La/Yb]_N ratios systematically decrease upward (14,600-2800 and 13-3.2, respectively) (Figure 4).

Unit b displays a slight reversal of trend for elements such as Rb, Nb, and Y (Figure 3). This reversal may be the result of a relatively large eruption that tapped a slightly deeper level of the Bandelier magma chamber. Indeed, unit b is a thick (2 m at section 15) Plinian deposit when compared with other Cerro Toledo Rhyolite tephra units. We believe significant the

1986 STIX ET AL.

TABLE 3b. Geochemical Analyses for Associated Rocks

Number	Toledo Ring Fracture Group					Turkey Ridge Group			Cerro Toledo Group			Southeast Rhyolite Group	
	Warm Springs Dome	Cerro Trasquiter	West Los Pozos	West Los Pozos	East Los Pozos	Indian Point	Unnamed Dome	Rabbit Mountain	Cerro Toledo	Unnamed Dome	Unnamed Dome	Unnamed Dome	Pinnacle Peak
	F82-9	F81-139	F81-123	F83-27	F83-26	F81-141	F83-28	F80-36	F81-145	F83-24	F83-29	F81-150	F81-159
SiO ₂	75.9	75.2	74.3	76.3	76.4	77.3	76.9	76.9	77.0	76.8	77.1	77.0	74.1
TiO ₂	0.05	0.08	0.12	0.12	0.12	0.09	0.08	0.08	0.08	0.07	0.08	0.08	0.07
Al ₂ O ₃	12.6	11.9	12.4	12.8	12.5	12.2	12.2	12.1	12.2	12.0	12.2	12.2	12.2
Fe ₂ O ₃	1.86	1.01	1.34	1.29	1.30	0.98	1.06	1.03	1.19	1.61	1.16	1.07	0.99
MnO	0.03	0.07	0.06	0.03	0.06	0.06	0.05	0.07	0.05	0.06	0.06	0.07	0.07
MgO	0.08	0.03	0.08	0.06	0.08	0.04	0.05	0.03	0.02	0.03	0.03	0.03	0.03
CaO	0.12	0.26	0.44	0.33	0.43	0.20	0.16	0.30	0.14	0.12	0.18	0.25	0.19
Na ₂ O	3.80	4.22	3.95	4.16	4.44	4.57	3.91	4.51	4.21	3.92	4.08	4.46	4.02
K ₂ O	4.94	4.49	4.62	4.54	4.40	4.57	4.54	4.42	4.47	4.43	4.53	4.43	4.40
P ₂ O ₅	0.02	0.005	0.01	0.005	0.01	0.005	0.005	0.005	0.005	0.005	0.01	0.005	0.14
LOI	0.89	3.19	3.53	0.46	0.46	0.28	0.52	0.59	0.25	0.33	0.21	0.50	3.11
Total	100.32	100.32	100.88	100.12	100.14	100.08	99.48	100.03	99.59	99.38	99.84	100.04	99.37
Cl	900	2000	1100	200	900	600	800	2100	800	600	300	2700	2100
Rb	298	208	139	143	143	176	182	195	199	197	198	202	199
Cs	11	8.1	3.7	3.6	3.8	4.9	4.5	6.9	4.6	4.1	4.1	8.6	7.8
Sr	6.6	<1	23	20	20	<1	<1	<1	<1	<1	2.3	<1	<1
La	32	36	57	40	44	40	36	43	31	27	28	34	41
Ce	76	80	89	...	91	71	70	83	72	69	70	68	73
Nd	19	29	33	26	31	28	56	23	18	25	15	23	28
Sm	8.3	7.4	7.7	6.8	5.8	7.7	8.2	8.7	7.0	5.3	7.1	7.4	9.0
Eu	0.06	0.09	0.14	0.14	0.19	0.08	...	0.10	...	0.07	...	0.11	0.08
Dy	16	12	8.0	6.2	6.9	8.4	8.8	11	10	7.4	7.9	12	12
Yb	11	8.1	4.8	4.4	5.0	5.7	5.9	7.9	5.7	5.7	6.0	6.8	7.7
Lu	1.4	0.97	0.59	0.65	0.67	0.72	0.67	1.0	0.74	0.80	0.75	0.85	0.93
Y	106	68	45	40	44	50	54	68	50	49	60	66	67
Zr	259	164	162	168	168	142	158	173	172	168	172	169	161
Hf	13	8.8	6.3	6.2	6.0	6.7	7.2	8.9	8.6	7.7	8.4	8.5	7.8
Nb	150	98	69	69	70	83	89	97	99	99	98	100	97
Th	34	23	19	21	19	21	22	22	23	24	23	24	23
U	16	8.2	5.9	5.9	6.1	6.6	7.6	8.0	8.5	8.6	7.7	8.4	8.1

SITE #1: RESTAURANT OF CONVENTIONAL ZONATION

Zr	259	164	162	168	168	158	173	172	168	172	169
Hf	13	8.8	6.3	6.2	6.0	7.2	8.9	8.6	7.7	8.4	8.5
Nb	150	98	49	69	70	89	97	99	99	98	100
Th	34	23	19	21	19	22	22	23	24	23	24
U	16	8.2	5.9	5.9	6.1	6.6	7.6	8.0	8.6	7.7	8.4

	Cerro Rubio Group			Tsankawi Pumice*				Lower Bandelier Tuff			Pre-Bandelier Pumices*		
	Cerro Rubio		Latite Plug F83-22	6-8†	6-9†	F82-94	F82-95	G-1‡	G-2‡	F82-11‡	F83-12‡	F82-91	F82-92
	F81-154	F83-245											
SiO ₂	66.9	66.9	68.2	72.7	67.4	73.6	74.2	73.0	74.4
TiO ₂	0.45	0.47	0.45	0.08	0.43	0.04	0.08	0.11	0.10
Al ₂ O ₃	15.1	15.2	15.5	11.5	11.9	12.2	15.0	11.4	11.8	11.9	11.8	12.0	11.8
Fe ₂ O ₃	3.04	3.43	3.55	1.56	2.12	1.47	3.20	1.48	1.54	1.40	1.50	1.25	1.54
MnO	0.05	0.05	0.06	0.09	0.09	0.08	0.06	0.08	0.09	0.07	0.05	0.06	0.06
MgO	1.31	1.42	1.29	0.05	1.35	0.10	0.09	0.42	0.08
CaO	3.25	3.32	3.23	...	0.99	0.33	3.19	0.41	...	0.24	0.30	0.45	0.33
Na ₂ O	3.70	3.60	3.96	3.95	3.83	3.08	4.86	3.94	4.25	4.36	2.86	2.90	4.00
K ₂ O	3.19	3.20	3.16	4.10	3.36	5.36	2.85	4.50	4.60	4.61	5.88	4.90	4.67
P ₂ O ₅	0.14	0.15	0.16	0.005	0.16	0.005	0.005	0.005	0.005
LOI	2.01	1.37	0.27	4.31	1.42	4.26	2.95	4.70	3.35
Total	99.13	99.11	99.83	99.37	99.92	100.59	99.72	99.80	100.34
Cl	600	400	...	2500	1900	2200	1140	2400	1900	2800	900	1100	1600
Rh	52	52	53	297	251	...	151	340	346	...	184	153	153
Cs	0.9	0.8	0.8	12	10	18	4.0	11	11	10	4.4	3.9	4.1
Sr	512	507	508	5.7	93	...	514	11	6.1	...	6.1	12	2.1
La	37	34	35	58	53	91	37	39	44	52	45	50	59
Ce	70	68	69	120	142	117	79	112	108	109	91	111	113
Nd	19	19	24	60	38	47	42	...	30
Sm	4.3	4.4	4.7	12	11	17	5.3	11	14	14	9.7	7.2	8.0
Eu	1.2	1.1	1.2	0.12	0.46	...	0.90	2.4	...	0.33	0.16
Dy	3.1	2.0	3.2	15	14	28	5.0	17	18	18	7.1	6.4	8.0
Yb	1.8	1.6	1.4	12	9.4	15	3.0	11	12	12	5.7	4.9	5.6
Lu	0.21	0.20	0.27	1.9	1.7	1.7	0.42	1.7	1.8	1.4	0.88	0.74	0.66
Y	18	18	18	113	100	...	31	112	111	...	55	45	47
Zr	228	226	228	205	273	...	229	256	278	...	186	209	231
Hf	5.4	5.0	4.8	14	13	14	6.6	13	12	12	6.7	8.4	8.2
Nb	13	12	13	156	133	...	32	191	212	...	83	71	71
Th	5.5	4.6	4.6	32	27	40	11	40	46	...	22	21	21
U	1.2	1.2	1.1	12	9.9	12	2.7	16	17	16	14	6.8	6.7

* Analyzed samples are combined pumice lapilli that were handpicked and cleaned ultrasonically prior to being crushed.

† Samples collected from section 6.

‡ Samples collected from Guaje Pumice at base of Lower Bandelier Tuff.

TABLE 4. Correlations Between Cerro Toledo Rhyolite Domes and Tephra

Dome	Tephra Unit
Warm Springs dome, Cerro Trasquilar (Southeast Rhyolite Group)	g
Warm Springs dome, Cerro Trasquilar (Southeast Rhyolite Group)	f
Southeast Rhyolite Group (Warm Springs dome, Cerro Trasquilar)	e, e'
Turkey Ridge Group	d
Turkey Ridge Group?	c, c'
Los Posos domes	b
Los Posos domes	b'

Domes in parentheses indicate a less favored, but possible correlation with the corresponding tephra unit. Question mark indicates an uncertain correlation.

fact that Rb, Nb, and Y are correlated and all show this chemical reversal.

Similarly, samples 6-8 and 6-9 show a reversal within the Tsankawi Pumice (Figures 3 and 4). The eruption that deposited the fall unit represented by sample 6-9 may have tapped deeper levels in a zoned magma chamber. Again, Rb, Nb, and Y show correlated trends. The extremely large jump in Sr content between the two units (5.7 to 93 ppm) is difficult to explain. The jump may be a manifestation of contamination and/or mixing of rhyolite magma with Tschicoma/Cerro Rubio dacite magma of high Sr content (about 507-512 ppm) (Gardner et al., 1986; Self et al., 1986). However, major elements, in particular K_2O , do not support a mixing model.

Sr trends are unclear, possibly because of analytical imprecision at relatively low Sr contents. Rb/Sr increases from unit b' upward (Rb/Sr 6.9-52) (Figure 4b). If unit d is incorrectly correlated and sample 15-11 is used instead of 6-6, Rb/Sr

increases from 5.8 to 52. Furthermore, unit b may represent a reversal of trend, as discussed above. If so, then Rb/Sr may increase upsection from unit b' to the Tsankawi (6.9-52).

Significance

We believe the chemical gradients documented here in the Cerro Toledo Rhyolite tephra represent successive liquid compositions at or near the top of the Bandelier magma chamber between 1.45 and 1.12 Ma. Four lines of evidence support this contention.

1. Cerro Toledo Rhyolite eruptions originated from point sources and produced fallout and surge tephra without associated large-scale pyroclastic flows. These eruptions were of relatively small volume ($<1 \text{ km}^3$) when compared with those that produced LBT and UBT ($>250 \text{ km}^3$) and most likely tapped only the upper surface of the magma [e.g., Druitt and Sparks, 1984].

2. Trace element concentrations of the Cerro Toledo Rhyolite tephra show consistent, systematic increases and decreases with respect to stratigraphic position. If the Cerro Toledo Rhyolite eruptions had tapped various levels of the compositional zonation instead of the uppermost level, chemostratigraphic variation would be random, not systematic.

3. Cerro Toledo Rhyolite tuffs and domes are generally crystal poor, consistent with these rocks being derived from the upper part of the magma chamber (Smith and Bailey, 1966; Smith, 1979).

4. When plotted on variation diagrams (see below), Cerro Toledo Rhyolite compositions exhibit both well-defined trends and alignment with samples of the Upper and Lower Bandelier Tuff. This suggests the Cerro Toledo Rhyolite and Bandelier magmas are comagmatic and tapped the same magma chamber.

With these points in mind, we now compare enrichment trends for LBT, UBT, and the interval of time during which

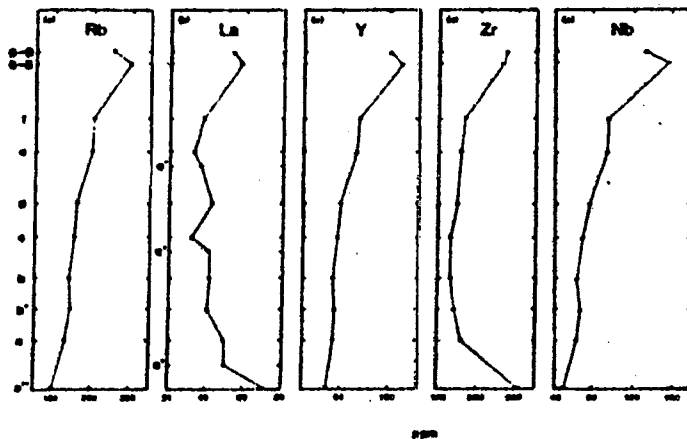


Fig. 3. Compositional variation with respect to stratigraphic height of selected trace elements within the Cerro Toledo Rhyolite tephra. The stratigraphically lowest and highest sampled units are a' and f, respectively. Units 6-8 and 6-9 refer to samples from the Tsankawi Pumice (UBT), which overlies the Cerro Toledo Rhyolite tephra. Analyzed samples of individual units are pumices except for units c' and e', which are fine-grained phreatomagmatic ashes. Individual units are represented by the following samples: a', 15-8; a', 14-7, 14-8; a, 15-9; b', 6-1; b, mean of 6-2, 6-3, 6-4; c, 6-5; c', 14-4, 15-3; d, 6-6; e, 6-7; e', 15-2, 25-1; f, 15-6; and Tsankawi Pumice, 6-8, 6-9. No vertical scale is shown because the tephra varies in thickness at different localities. Compare with Smith [1979, Figure 8] and Mahood [1981, Figures 4 and 5].

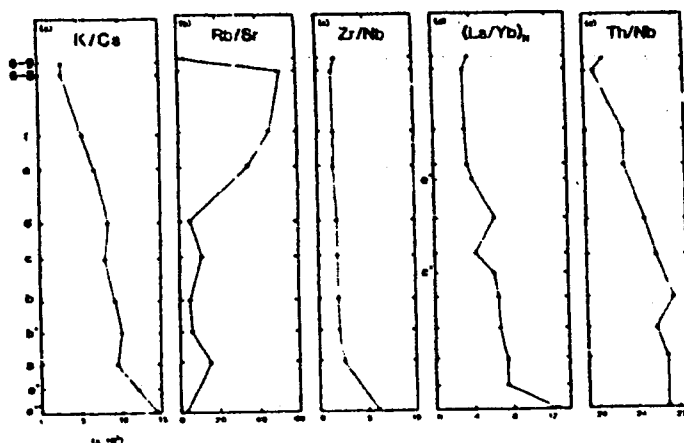


Fig. 4. Variation of major and trace element ratios with respect to stratigraphic height in the Cerro Toledo Rhyolite tephra. Unit names and sample numbers are the same as those listed in Figure 3.

the Cerro Toledo Rhyolite was erupted between the two ignimbrite sequences (Figure 5). The enrichment ratios represent the concentration of a particular element in the earliest erupted material divided by the concentration in the last-erupted deposits [cf. Hildreth, 1979]. We again stress the important distinction between the Cerro Toledo Rhyolite and Bandelier Tuff; whereas the Cerro Toledo Rhyolite represents small eruptions that tapped the top of the magma chamber over a period of 0.27–0.33 m.y., the LBT and UBT are the result of viscerating eruptions that sampled the chemical stratigraphy present in the magma chamber at an instant in geologic time [Hildreth, 1981]. The data for the interval between the LBT and UBT are taken from the stratigraphically lowest sampled Cerro Toledo Rhyolite (15-8) and basal Tsankawi unit (6-8). We have chosen the UBT sample instead of that from the stratigraphically highest Cerro Toledo Rhyolite tephra unit (unit 7) for two reasons: (1) we want to document compositional changes at the top of the Bandelier magma chamber during the 0.33-m.y. period between the two caldera-forming eruptions; however, the Cerro Toledo Rhyolite tephra sequence does not fully record these changes; and (2) systematic compositional changes occur from the base of the Cerro Toledo Rhyolite tephra to the base of the UBT (Figures 3 and 4); thus we have considered sample 6-8 as a logical end-member of the Cerro Toledo Rhyolite tephra sequence.

Figure 5 shows geochemical trends for the intracaldera interval opposite to those displayed by LBT and UBT, with respect to Rb, Y, Nb, and Th. The trends suggest that chemical gradients were restored between the two ignimbrite eruptions [Smith, 1979]. If we take 0.33 m.y. as the age range of intracaldera volcanic activity, we can calculate the rate of restoration of compositional zonation at the top of the Bandelier magma chamber. For Rb, Y, and Nb, the rates are 0.60 ppm kyr⁻¹, 0.23 ppm kyr⁻¹, and 0.32 ppm kyr⁻¹, respectively. For comparison, Nb enrichment in Cerro Toledo Rhyolite TRF domes increased at an average rate of 0.32 ppm kyr⁻¹ (Tables 1 and 3). Furthermore, Smith [1979, Figure 8] shows a rate of 0.35 ppm Nb kyr⁻¹, and we calculate a rate of 0.34 ppm Nb kyr⁻¹ using data from Balsley et al. [1985] and Kuentz et al. [1985]. Due to stratigraphic and age uncertainties, there is a

certain degree of error in these calculations. As order-of-magnitude estimates, however, we believe they are correct.

Figure 5 indicates that the magnitude of early/late intracaldera depletion of Rb, Nb, and Y resembles that of LBT enrichment much more closely than UBT. This implies that the extent of chemical zonation reestablished in intracaldera time equalled that tapped by the LBT eruption. The UBT eruption may not have tapped the zoned magma chamber to the extent that the LBT eruption did. This explanation is consistent with the smaller volume of UBT (250 km³) compared with LBT (400 km³) [Balsley et al., 1985, 1986; Kuentz et al., 1985].

PETROGENESIS

Crystal Fractionation

We believe that crystal fractionation has generated certain of the chemical gradients in the Cerro Toledo Rhyolite, as well as in the Bandelier Tuff. We present here data that support this hypothesis. We utilize two types of diagrams in the following discussion.

1. Chemostratigraphic plots that show changes in chemistry with respect to stratigraphic height and time (Figures 3 and 4).

2. Bivariant plots with Nb plotted as the abscissa (Figures 6 and 8–11). Although Nb clearly is fractionated, we justify this choice because (1) Nb appears relatively incompatible (but not to the extent of Cs; see below) in the Cerro Toledo Rhyolite and Bandelier Tuff rocks as shown in Figure 6, where Nb varies linearly with Rb, and the Rb/Nb ratio remains essentially constant at 2 above 50 ppm Nb; (2) Nb has far better relative precision than does Cs at the concentration levels encountered in these rocks (Table 2); (3) we use Nb as an index of magmatic evolution following Smith [1979, Figure 8]; and (4) Nb is relatively immobile [Pearce and Norry, 1979].

Feldspar fractionation. Figures 7 and 8 show depletions of K/Cs and Sr with increasing Cs and Nb, respectively. These are general trends for rocks of different ages but also are reflected in the Cerro Toledo Rhyolite points. The youngest Cerro Toledo Rhyolite tephra tend to be most depleted in

unit 6 may represent a
of so, then Rb/Sr may
of (6.9–52).

documented here in the
successive liquid com-
plexer magma chamber
evidence support this

originated from point
tephra without associ-
ated eruptions were of
compared with those
km³) and most likely
magma [e.g., Dravit and

of the Cerro Toledo
natic increases and de-
position. If the Cerro
at various levels of the
the uppermost level,
random, not system-

d domes are generally
as being derived from
er [Smith and Bailey,

ams (see below). Cerro
both well-defined trends
er and Lower Bandel-
er Rhyolite and Bandel-
er the same magma

compare enrichment
of time during which

Cerro Toledo
4 and 6-9 refer
and samples of
vidual units are
e.g., 14-4, 15-3;
tephra varies in

6139 STIX ET AL.

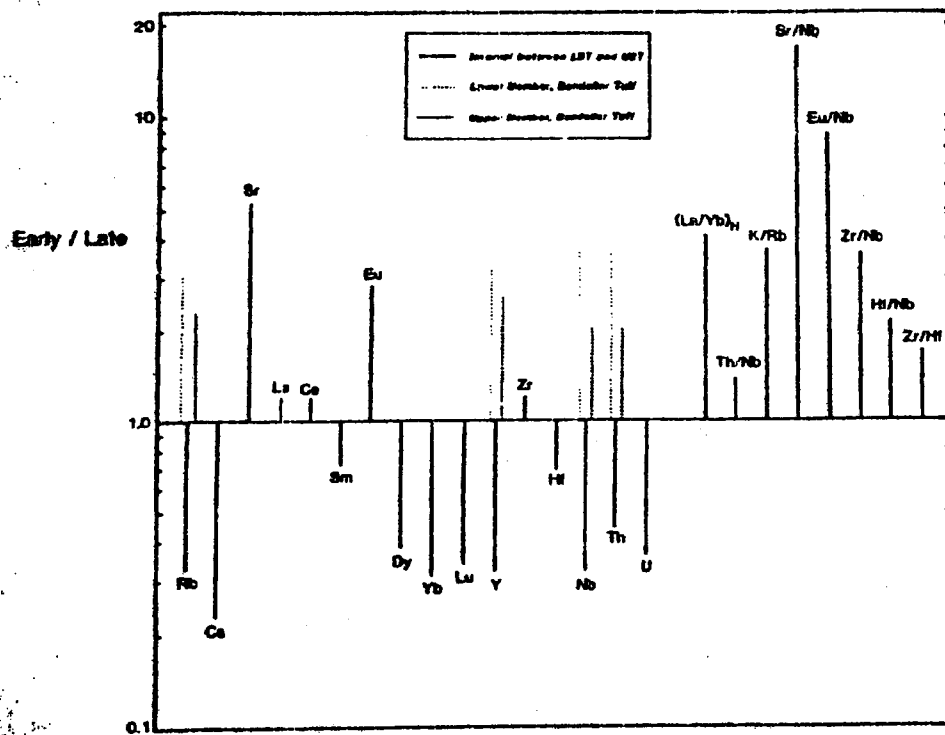


Fig. 5. Early/late enrichment-depletion trends for the interval, indicated by the solid lines, between the LBT and UBT caldera-forming eruptions. The data simply represent concentrations of trace elements in unit *a** (sample 15-8) at the base of the Cerro Toledo Rhyolite divided by the concentrations in the Tsankawi Pumice of the Upper Member of the Bandelier Tuff (sample 6-8) which overlies the Cerro Toledo Rhyolite tephra. In contrast to similar diagrams constructed from ignimbrite data [e.g., *Hildreth, 1981, Figure 7*], this diagram has evolutionary significance and spans approximately 0.33 m.y. [see also *Mahood, 1981, Figure 6*]. For comparison, we also have plotted on this diagram early/late enrichment factors for Rb, Y, Nb, and Th from the lower and upper members of the Bandelier Tuff [*Balslev et al., 1985; Keenly et al., 1985*]. As stated above, these enrichment factors have no rate significance because the ignimbrites were erupted geologically instantaneously. The enrichment factors represent compositions of earliest erupted basal pumice falls from each ignimbrite cycle divided by the compositions of pumices in the last-erupted ignimbrite of the particular cycle.

K/Cs) and Sr, suggesting feldspar fractionation has removed K and Sr relative to Cs and Nb in successive magmas.

Figures 4a and 4b also display these relations. K/Cs and Rb/Sr decrease and increase upsection, respectively. Changing proportions of feldspar during the crystallization process resulted in variable amounts of Sr in the residual magma as represented by the Cerro Toledo Rhyolite tephra. In spite of the large chemostratigraphic fluctuations of Sr, Rb/Sr increases upsection from 3.3 at unit *a** (base of Cerro Toledo Rhyolite) to 22 at unit 6-8 (base of UBT). Because an element such as Rb is continually enriched during the crystallization process because of its relative incompatibility, crystallization of varying amounts of feldspar will result in an increasing Rb/Sr ratio upsection. The Rb/Sr ratio will remain constant only if feldspar fractionation ceases completely so that Sr becomes incompatible to the extent of Rb.

Zircon fractionation. When plotted against Nb, Zr shows a wide scatter of points that defines no broad relationship (Figure 5b). Zr generally increases in concentration with Nb for Cerro Toledo Rhyolite tephra. In contrast, Zr/Nb is strongly depleted with increasing Nb, particularly for Cerro Toledo Rhyolite tephra in which the youngest tephra are

most depleted (Figure 9b). These relations and the presence of zircon in Cerro Toledo Rhyolite tephra suggest zircon fractionation.

Chemostratigraphic diagrams show an initial decrease, followed by increase, of Zr upsection (Figure 3d). However, Zr/Nb progressively decreases upsection from 6.2 at unit *a** to 1.7 at unit 6-9 (Figure 4c). This implies that zircon fractionation occurred throughout Cerro Toledo Rhyolite time from a magma that remained saturated in zircon. From unit *a** to *c*, zircon fractionation was sufficient to deplete the residual magma of both Zr and Zr/Nb; the bulk distribution coefficient of Zr exceeded unity. From unit *c* upsection, Zr increases (135-273 ppm) but Zr/Nb decreases (2.0-1.7), perhaps due to less zircon fractionation. The bulk distribution coefficient of Zr may have decreased to below 1; zircon fractionation still took place, however, because the Zr/Nb ratio decreases progressively upsection. It is probable that zircon was crystallizing in different proportions in different parts of the magma chamber, because (1) zircon saturation is sensitive to small changes in temperature and water content of the magma [*Watson and Harrison, 1983, 1984*] and (2) the magma chamber was zoned with respect to temperature and volatiles

[*Stey et al., 1985*]. The increase of Zr/Nb from 6.2 at unit *a** to 1.7 at unit 6-9 is consistent with a magma that remained saturated in zircon and that the Zr/Nb ratio increased because of zircon fractionation.

Fractionation of Zr/Nb is plotted against Nb for Cerro Toledo Rhyolite tephra (Figure 5b) and compared to the correlation of Zr/Nb versus Nb for Cerro

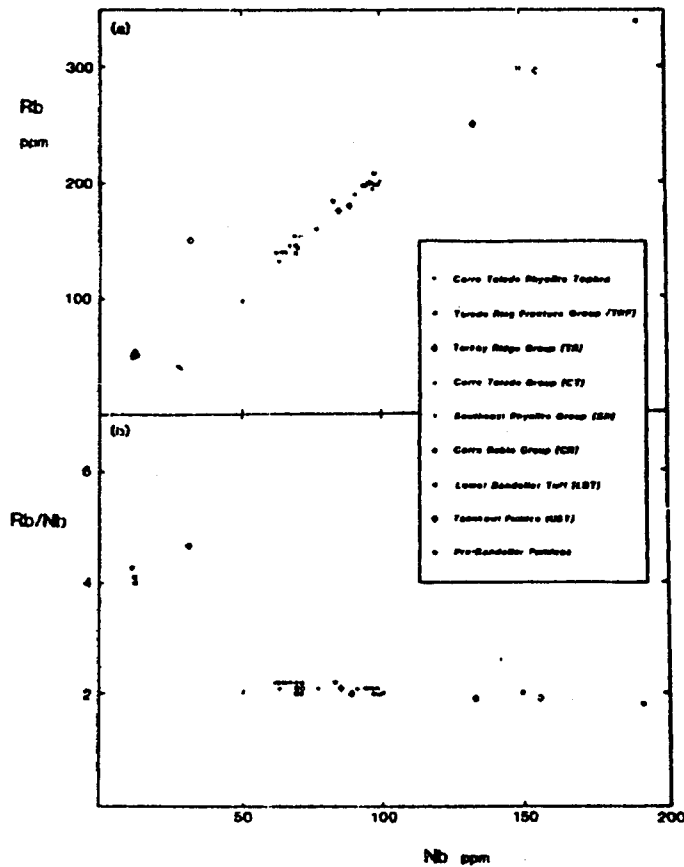


Fig. 6. (a) Nb plotted against Rb in ppm. A well-correlated linear trend is apparent. Cerro Toledo Rhyolite tephra samples that are most enriched in Nb and Rb represent the later stages of Cerro Toledo Rhyolite intracaldera explosive volcanism. Cerro Rubio Group samples are relatively depleted in Nb and Rb. (b) Nb versus Rb/Nb. The Rb/Nb ratio remains relatively constant above 50 ppm Nb. The symbols in this diagram remain the same in the following figures.

[Smith and Bailey, 1966; Warsaw and Smith, 1980]. Notably, the increase in chlorine content mimics that of Zr from unit f (sample 15-6) to the base of the Tsankawi Pumice (sample 6-8). Zr increases by 58% from 168 ppm in unit f to 265 ppm in the Tsankawi Pumice (Figure 3d), whereas Cl increases from 1700 to 2500 ppm (47%) over the same interval. If Cl contents are indicative of overall volatile concentrations in the magma chamber, these trends suggest that volatile contents (1) control, at least in part, zircon saturation in the magma and (2) increased significantly in the Bandelier magma chamber before the eruption of the Upper Member of the Bandelier Tuff.

Fractionation of an LREE-rich accessory phase. When plotted against Nb, La displays wide scatter in which Cerro Toledo Rhyolite points show La depletion: with increasing Nb (Figure 10a). However, $[La, Yb]_n$ is strongly depleted with respect to Nb, particularly for the Cerro Toledo Rhyolite (Figure 10b). Although Th and Nb show a positive linear correlation, Th/Nb also decreases with Nb enrichment (Figure 11). For Cerro Toledo Rhyolite tephra, the oldest are most

depleted in Th but have the highest Th/Nb values, similar to Zr relations in Figure 9. These trends contrast with those of Figure 6, in which Nb and Rb are positively correlated with essentially no change in the Rb/Nb ratio above 50 ppm Nb. These data suggest fractionation of a phase that has preferentially incorporated both Th and LREE. In metaluminous rocks, allanite is an accessory mineral that contains LREE as essential constituents [Rapp et al., 1986]. Allanite is an accessory phase in unit a' of the Cerro Toledo Rhyolite tephra [Heiken et al., 1986], in the Bandelier Tuff [Kuentz, 1986], and in the Valles Rhyolite of post-Valles caldera age (T. Spell, New Mexico Institute of Mining and Technology, personal communication, 1987). We have plotted theoretical Rayleigh fractionation trends for allanite in Figures 10 and 11 by assuming crystallization of 0.06–0.08 wt % allanite from sample 15-8 as the parent. There is reasonable agreement between the theoretical and observed curves, despite mineral proportions and partition coefficients that are poorly constrained. Because allanite is so efficient at extracting LREE from the magma, however, the exact values of the partition coefficients for each

and the presence of
to suggest zircon frac-
initial decrease, fol-
Figure 3d). However,
from 6.2 at unit a' to
that zircon frac-
Toledo Rhyolite time
in zircon. From unit
at 40, deplete the re-
the bulk distribution
unit c' upsection. Zr
rises (2.0–1.7), per-
the bulk distribution
below 1; zircon frac-
the Zr/Nb ratio
probable that zircon
in different parts of
saturation is sensitive
later content of the
) and (2) the magma
erature and volatiles

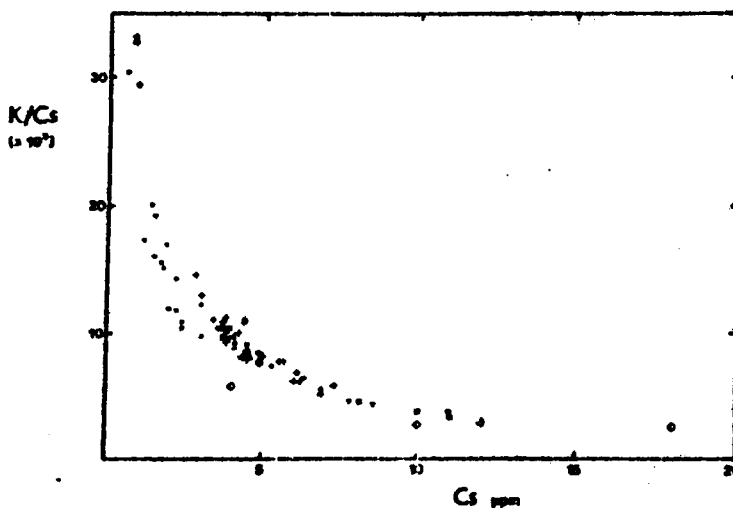


Fig. 7. Cs versus K/Cs. The data indicate decline of K/Cs with increasing Cs, both overall (K/Cs $33\text{--}2.5 \times 10^3$) as well as for samples of Cerro Toledo Rhyolite tephra (K/Cs $15\text{--}3.2 \times 10^3$). Symbols as in Figure 6, except for the stars, which indicate Tachicoma Formation andesites and dacites (Loeffler, 1984). These intermediate rocks, erupted at 3.7–6.7 Ma, are similar in age and composition to Cerro Rubio and may represent parental magmas of the Cerro Toledo Rhyolite and Bandelier Tuff.

element are of secondary importance. The partitioning ratios between individual REE are significant when modeling elemental ratios such as La/Yb and Th/Nb.

Chemostratigraphic data show general decreases upsection for both $[\text{La}/\text{Yb}]_n$ and $[\text{Th}/\text{Nb}]_n$ (Figures 4d and 4e). $[\text{La}/\text{Yb}]_n$ decreases fourfold (13–3.2) from unit 8* to 6–8, whereas $[\text{Th}/\text{Nb}]_n$ decreases only 1.4 times over the same interval. $[\text{La}/\text{Sm}]_n$ shows a decrease similar to $[\text{Th}/\text{Nb}]_n$ (1.7 times). Enhanced depletion of La compared with Th and Sm possibly results from the greater compatibility (threefold to sixfold) of La over Th and Sm into a phase such as allanite due to charge and size differences (Brooks et al., 1981; Mahood and Hildreth, 1983). Th may be partitioned into zircon as well, but the partition coefficient is 4.6–8.8 times smaller than that of allanite in high-silica rhyolites (Mahood and Hildreth, 1983). As with Zr, La contents increase significantly (53%) from unit 1 (38 ppm) to the Tachicoma Pumice (58 ppm) (Figure 3a). Chlorine contents increase 47% over the same interval, implying that volatile contents may control the solubility of LREE-enriched accessory phases in the magma.

Similar studies have shown that LREE depletion in nonperalkaline silicic magmas occurs frequently. Gromet and Silver (1983) have presented convincing evidence that the REE content of the melt in a granodiorite pluton decreased substantially during early crystallization of allanite and apatite. Miller and Mittelscheldt (1982), Mittelscheldt and Miller (1983), and Barst (1986) have suggested that accessory phases such as monazite and allanite can effectively remove significant quantities of LREE because these elements are stoichiometric constituents of the minerals. Clearly, the ability of monazite and allanite to deplete a melt of its LREE attests to the low solubility of these accessory phases in nonperalkaline silicic melts (Rapp and Watson, 1986; Rapp et al., 1986).

Apatite fractionation. The very low P_2O_5 contents of the Cerro Toledo Rhyolite domes (generally $<0.14\%$ P_2O_5) sug-

gest that apatite was removed from the magma (Watson, 1979; Watson and Capobianco, 1981). Because the solubility of apatite decreases significantly (to about 0.14% P_2O_5 in rhyolite) with increasing silica content, the Cerro Toledo Rhyolite magmas clearly were once saturated in apatite and crystallized apatite (Watson and Capobianco, 1981). However, apatite cannot have fractionated significant LREE from the melt because (1) LREE are not essential structural constituents of apatite, and thus the bulk distribution coefficients of LREE due solely to apatite are ≈ 1 ; (2) apatite does not preferentially incorporate LREE over middle rare earth elements (MREE) and HREE (Arita, 1976; Watson and Green, 1981); and (3) P_2O_5 contents in even the least fractionated samples are so low that not much apatite crystallization is likely to have taken place ($<0.3\%$).

"Incompatible" elements. From the evidence presented above, we believe that crystal fractionation is an important, perhaps dominant, process in the evolution of the Cerro Toledo Rhyolite and Bandelier magmas. We begin with the Rayleigh equation:

$$C_L/C_0 = F^{D-1} \quad (1)$$

where C_0 is the concentration of an element in the parental liquid, C_L the concentration of the element in the residual liquid as a result of fractional crystallization, F the amount of liquid remaining after crystallization, and D the bulk distribution coefficient. For incompatible elements, $D < 1$; therefore (1) can be rewritten in the form

$$C_L/C_0 = F^{-1} \quad (2)$$

or

$$C_0/C_L = F \quad (3)$$

This simple inverse approach to petrogenetic modeling (Alb-

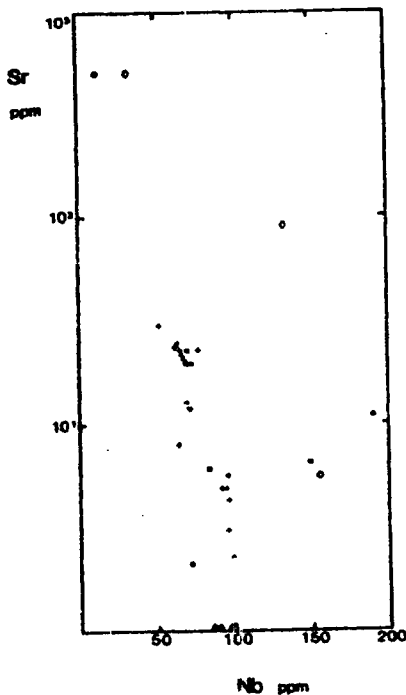


Fig. 8. Semilog plot of Nb versus Sr. The data suggest rapid depletion of Sr with increasing Nb, particularly for Cerro Toledo Rhyolite tephra. Many Cerro Toledo Rhyolite domes contain practically no Sr. Note (1) the Tsankawi Pumice sample that contains 514 ppm Sr (FR2-95) plotted near the Cerro Rubio Group samples, and (2) the four points, all above 130 ppm Nb, that fall off the overall trend and are relatively enriched in Sr for such high concentrations of Nb. Only one of these points is a Cerro Toledo Rhyolite. See text for discussion. Symbols as in Figure 6.

... the magma [Watson, because the solubility of ... 0.14% P_2O_5 in rhyolite Cerro Toledo Rhyolite ... apatite and crystal ... 1981]. However, apatite and LREE from the melt ... structural constituents of ... elements of LREE ... not preferentially ... elements (MREE ... 1981); and (3) ... samples are so ... zonation is likely to have ... the evidence presented ... onation is an important ... evolution of the Cerro ... We begin with the ... (1) ... element in the parental ... element in the residual ... zonation. F the amount of ... and D the bulk distri- ... elements, $D \ll 1$; therefore ... (2) ... (3) ... genetic modeling [All-

between each other (Figure 6), and (3) the estimate of 78% crystallization from the Cs data represents a minimum figure. Although less compatible than Rb because of its large size, Cs does enter alkali feldspar to a certain degree [Nash and Crafts, 1985]. Thus the amount of crystallization was probably higher.

We explore below physical processes that may or may not be capable of (1) forming the chemical gradients we have documented for the Cerro Toledo Rhyolite, (2) enriching the residual magma severalfold in incompatible trace elements [Miller and Mittlefehdt, 1984], and (3) generating nearly aphyric liquids as represented by the Cerro Toledo Rhyolite.

Connective fractionation. Recent experimental and theoretical work suggests that sidewall crystallization could result in the formation of a compositionally light, incompatible-element-enriched boundary layer that flows up the walls of the magma chamber to stratify at the top [Sparks et al., 1984]. As well, solidification at the roof may result in a crystallization front that moves downward into the magma chamber with time [Baker and McBirney, 1985]. This is essentially in situ crystallization. We favor roofward crystallization over sidewall crystallization for the following reasons: (1) heat loss is greatest at the roof [Irvine, 1970]; (2) stratification by roofward crystallization may be more efficient than sidewall crystallization because the light boundary layer formed by the latter process may be affected by shearing, backmixing [McBir-

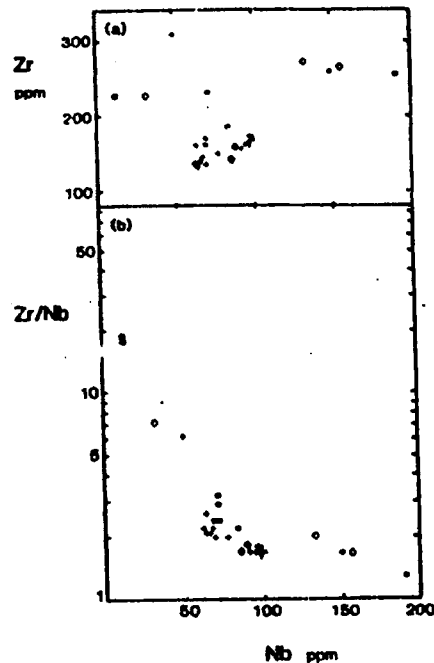


Fig. 9. (a) Nb versus Zr. A wide scatter of points is exhibited for the various groups. There is a poorly defined increase in Zr with Nb for Cerro Toledo Rhyolite tephra samples. (b) Semilog plot of Nb versus Zr/Nb. Zr/Nb decreases with increasing Nb. In contrast to Figure 9a, Cerro Toledo Rhyolite tephra samples show a general decrease in Zr/Nb with increasing Nb. The four points above 130 ppm Nb, only one of which represents the Cerro Toledo Rhyolite, fall off the trend of Zr/Nb depletion. Symbols as in Figure 6.

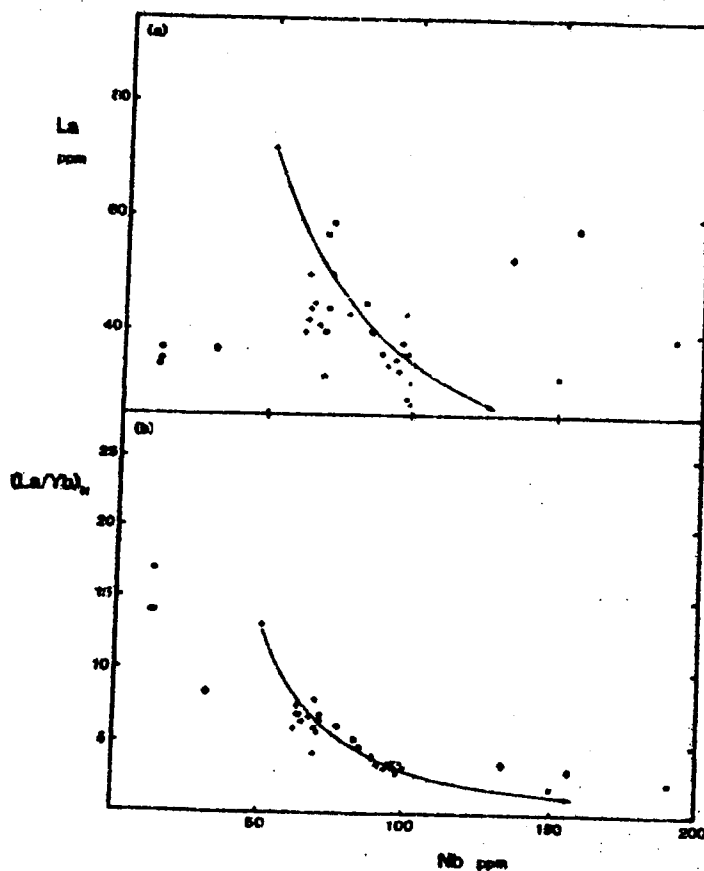


Fig. 10. (a) Nb versus La. A wide scatter of points is indicated for the different groups. (b) Nb versus $[La/Yb]_0$. $[La/Yb]_0$ is depleted with increasing Nb. A break in slope occurs above 130 ppm Nb, where four samples are relatively enriched in $[La/Yb]_0$, compared with the other data points, for the appropriate Nb concentration. Only one of these four points is a Cerro Toledo Rhyolite. The dashed lines are theoretical Rayleigh fractionation curves for allanite. Sample 15-4 just above the base of the Cerro Toledo Rhyolite represents the parental Cerro Toledo Rhyolite magmas at 50 ppm Nb, and the direction of fractionation is indicated by the arrows. Our chosen theoretical values for allanite are 0.0008 weight fraction allanite, $D_{La} = 2394$, $D_{Yb} = 31$, and $D_{Nb} = 3$ (Mahood and Hildreth, 1983). Symbols as in Figure 6.

may be a 1985), interference by growing crystals [Huppert and Sparks, 1984, p. 26], or other processes of disruption as it travels upward along the sidewalls before accumulating at the roof; and (3) the crystallization front at the roof remains in contact with the lightest, most fractionated liquid at the top of the magma chamber and further enriches and stratifies this liquid by continued crystallization. This systematic temporal change in the erupted products (i.e., the Cerro Toledo Rhyolite) may be ascribed to the changing composition with time of the most fractionated liquid at the top of the magma chamber.

Removal of crystals. The often-observed decreases of Zr and LREE in silicic magmas imply not only crystallization of zircon and LREE-enriched accessory phases but their removal from the residual liquid, as well. For a 100- μ m-diameter zircon crystal to settle 500 m in silicic magma at 785°C [Mahood, 1967] requires 1.2×10^5 years in magma with 5%

H₂O ($\eta = 10^6$ P) and 1.2×10^{11} years in anhydrous magma ($\eta = 10^{12}$ P), calculated using Stokes law. Except for very wet magmas, the settling times appear unrealistic compared with the duration of Cerro Toledo Rhyolite intracaldera activity ($2.7\text{--}3.3 \times 10^3$ years). Accessory phases also may be removed as inclusions in ferromagnesian phases such as biotite [Miller and Mittlefehldt, 1982, 1984; Cameron and Cameron, 1986]; however, biotite will not settle readily in silicic magma. Most logically, these crystals will be accreted to the margins of the magma chamber where heat loss is greatest, i.e., the roof of the chamber.

Assimilation

Melting the roof of a magma chamber also can produce compositionally light melts that stratify at the top of the chamber. So long as heat is supplied to the liquid at the top of

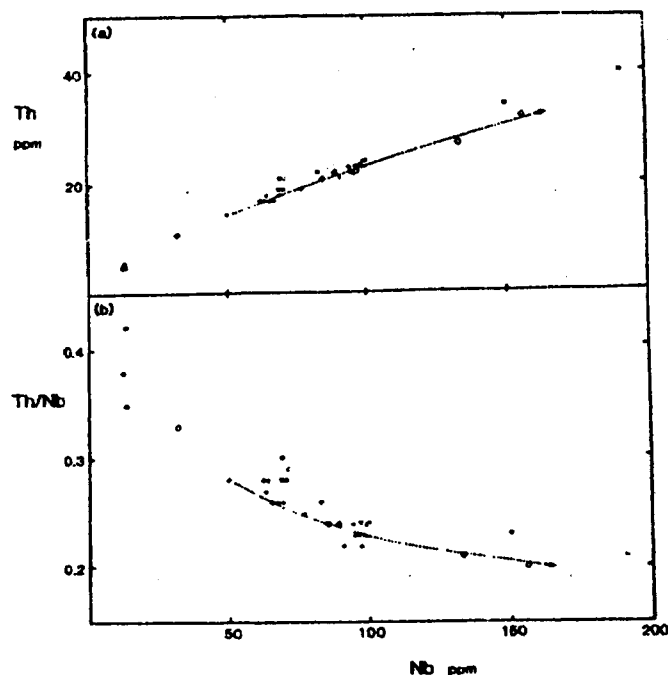


Fig. 11. (a) Nb versus Th. A well-correlated linear increase in Th with respect to Nb is indicated. (b) Nb versus Th/Nb. Th/Nb is depleted with increasing Nb. The change in slope for Cerro Toledo Rhyolite samples between Figures 11a and 11b is well illustrated. Theoretical curves are as described in Figure 10, except for 0.0006 weight fraction allanite and $D_{Th} = 484$. The discrepancy in weight fractions between this and Figure 10 is probably due to uncertainties in the partition coefficients for La and Th. Symbols as in Figure 6.

maintain superheat and prevent crystallization, roof melting will occur if the temperature of the magma exceeds the melting point of the wall rocks [Turner and Campbell, 1986]. The supply of heat may come from crystallization of mafic magma at a lower level in the magma chamber [Hildreth, 1981]. Theoretically, roof melting provides a more efficient mechanism than sidewall crystallization to stratify liquids at the top of the chamber; and roof melting combined with subsequent fractional crystallization may be a common process [Turner and Campbell, 1986]. It is difficult to assess the role of roof melting for Cerro Toledo Rhyolite magmas because of a lack of isotopic data; however, the following points suggest that roof melting was not responsible for the observed chemical variations: (1) Sr contents generally are very low in Cerro Toledo

Rhyolite rocks, and (2) Sr is strongly depleted with respect to Nb and follows a fractional crystallization trend (Figure 8). Fractional crystallization also may mask the effects of earlier roof melting. Isotopic data from the Bishop Tuff, a high-silica rhyolite that has many geochemical similarities with the Banded system, indicate that little or no melting of the roof occurred [Halliday et al., 1984]. In contrast, Noble and Hedge [1969] have shown that the first-erupted rocks of certain ash flow sheets have higher initial strontium ratios than do the later-erupted, upper parts of the sheets, indicating that the upper parts of the magma chambers were contaminated, possibly by roof melting, stoping, and/or fluid assimilation.

Diffusive and Soret Processes

Several workers have proposed liquid-state thermodynamic processes to explain observed major and trace element variations in ignimbrites [e.g., Hildreth, 1979, 1981; Schott, 1983]. We discuss, in turn, rates of diffusion among cations of different valencies and the Soret effect in silicic liquids.

For cations of similar ionic radius (K^+ , Ba^{2+}) at 800°C, diffusivity of the 2+ cation is 3 orders of magnitude lower than that of the 1+ [Hofmann, 1980 Figure 7]. Similarly, for Ca^{2+} and Ce^{3+} at 800°C, diffusivity of the 3+ cation is 6 orders of magnitude lower than that of the 2+ [Jambon, 1982, Figure 2]. Extrapolation suggests that diffusivities for 5+ cations such as Nb are much lower still [Jambon, 1982, equations (13) and (14)] (Table 6). Thus if diffusion played a significant role, Rb and Nb should be very strongly fractionated with

TABLE 5. Apparent F Values

Element	F
Cs	0.22
Yb	0.31
Y	0.32
Nb	0.32
Rb	0.33
Lu	0.34
U	0.36
Dy	0.38
Th	0.44

F is calculated by dividing concentration of sample 158 (C_0) by that of 6-8 (C_1), where $F = C_0/C_1$.

$[La/Yb]_0$
: four
: 15-8
at 20 ppm Nb,
is 0.0006 weight

in anhydrous magma
w. Except for very wet
realistic compared with
the intracaldera activity
is also may be removed
such as biotite [Miller
and Cameron, 1986];
in silicic magma. Most
ed to the margins of the
latest, i.e., the roof of the

rober also can produce
ability at the top of the
o the liquid at the top to

TABLE 6. Calculated Diffusivities for Three Cations of Different Valence State

Cation	Valency	Ionic Radius A	Activation Energy, kcal mol ⁻¹	Frequency Factor, cm ² s ⁻¹	Diffusivity, cm ² s ⁻¹
Rb	+1	1.52	23.5	2.3 × 10 ⁻³	2.4 × 10 ⁻⁷
Y	+3	0.90	77.0	5.0 × 10 ³	2.8 × 10 ⁻¹³
Nb	+5	0.64	488	6.3 × 10 ⁴⁴	6.5 × 10 ⁻⁵⁹

Diffusivities calculated from equations (13) and (14) of Jambon [1982] at 800°C. Ionic radii from Shannon [1976] in octahedral (VI) coordination.

respect to each other in Cerro Toledo Rhyolite and Bandelier rocks. However, Rb and Nb clearly are not fractionated (Figure 6).

Turning to the role of Soret diffusion, major and trace element fractionation in experimental felsic silicate melts by Soret processes contrasts strongly with geochemical gradients observed in certain ignimbrite sequences [cf. Smith and Bailey, 1966, Figure 16; Crecraft et al., 1981, Figure 6; Hildreth, 1981, Figure 7; Mahood, 1981, Figure 3; this work, Figure 5]. Leasher [1986, Figures 4c and 4d] has shown that network-forming elements (e.g., Si) fractionate to the hot end of the laboratory Soret temperature gradient, whereas network modifiers (e.g., Ca, Mg, Fe, and most trace elements) concentrate at the cold end, for silicic melt compositions at 1300°–1670°C. Ponader and Mahood [1984] have obtained similar results at temperatures more appropriate to silicic magmas (1030°C). These results conflict directly with ignimbrite data and suggest that Soret diffusion does not cause the compositional zoning documented in many silicic magma chambers.

CONCLUSIONS

We have reached four main conclusions from our study of the Cerro Toledo Rhyolite.

1. The Cerro Toledo Rhyolite tracks the restoration of compositional gradients at the top of the Bandelier magma chamber between 1.45 and 1.12 Ma.
2. Crystal fractionation was the major process by which these gradients were restored, mainly by crystallization at the roof of the magma chamber.
3. No one trace element which we have analyzed remained truly incompatible during evolution of the Cerro Toledo Rhyolite; Cs comes closest.
4. Diffusive and Soret processes did not contribute to any significant extent in forming the compositional zoning of the magma chamber.

Acknowledgments. We thank Roland Hagan, Isabel Laurence, John Wolff, Jamie Gardner, Greg Valentine, and Paul Carroll for assistance during various stages of the project. The second author thanks Joe Harrell of Boca Land and Cattle Co., Abilene, Texas, for access to the northern Valles caldera region during 1981–1984. Thorough reviews by Wes Hildreth and John Sturmer and comments by W. P. Nash have improved the manuscript substantially. This work is a contribution to the Thermal Regimes program of the U.S. Continental Scientific Drilling Project at Valles caldera. This study was supported by the Office of Basic Energy Sciences, U.S. Department of Energy, and the Natural Sciences and Engineering Research Council of Canada.

REFERENCES

- Abbey, S. Studies in "standard samples" of silicate rocks and minerals, 1969–1982, *Geol. Surv. Can. Pap.*, 83-15, 1–114, 1983.
- Aldrich, M. J. Tectonics of the Jemez lineament in the Jemez Mountains and Rio Grande rift, *J. Geophys. Res.*, 91, 1753–1762, 1986.
- Albarede, C. J., M. Treuil, J.-F. Minster, B. Minster, and F. Albarède. Systematic use of trace element in igneous process. I. Fractional crystallization processes in volcanic suites, *Contrib. Mineral. Petrol.*, 66, 57–75, 1977.
- Arth, J. G. Behavior of trace elements during magmatic processes—A summary of theoretical models and their applications, *J. Res. U.S. Geol. Surv.*, 4, 41–47, 1976.
- Bailey, R. A., R. L. Smith, and C. S. Ross. Stratigraphic nomenclature of volcanic rocks in the Jemez Mountains, New Mexico, *U.S. Geol. Surv. Bull.*, 1274-P, 1–19, 1969.
- Baker, B. H., and A. R. McBirney. Liquid fractionation. III. Geochemistry of zoned magmas and the compositional effects of liquid fractionation, *J. Volcanol. Geotherm. Res.*, 24, 55–81, 1985.
- Bailey, S. D., J. A. Wolff, J. N. Gardner, D. C. Kuentz, P. R. Kyle, and S. Sell. Compositional variations within the Upper Bandelier Tuff, Jemez Mountains, New Mexico, *Eos Trans. AGU*, 68, 1143–1143, 1985.
- Bailey, S. D., D. C. Kuentz, J. A. Wolff, and P. R. Kyle. Geochemistry of a large-volume high-silica rhyolite magma system associated with the Rio Grande rift: The Bandelier Tuff, New Mexico, *Geol. Soc. Am. Abstr. Programs*, 18, 533, 1986.
- Barritt, S. D. Evolution of radioactive-bearing accessory minerals and the distribution of U and Th in the Cairngorm Granite, eastern Scotland, *Eos Trans. AGU*, 67, 387, 1986.
- Brooks, C. K., P. Henderson, and J. G. Ronsbo. Rare-earth partition between allanite and glass in the obsidian of Sandy Braes, northern Ireland, *Mineral. Mag.*, 44, 157–160, 1981.
- Cameron, K. L., and M. Cameron. Whole-rock/groundmass differentiation trends of rare-earth elements in high-silica rhyolites, *Geochim. Cosmochim. Acta*, 50, 759–769, 1986.
- Crecraft, H. R., W. P. Nash, and S. H. Evans. Late Cenozoic volcanism at Twin Peaks, Utah: Geology and petrology, *J. Geophys. Res.*, 86, 10,303–10,320, 1981.
- Doell, R. R., G. B. Dalrymple, R. L. Smith, and R. A. Bailey. Paleomagnetism, potassium-argon ages, and geology of rhyolites and associated rocks of the Valles caldera, New Mexico, *Mem. Geol. Soc. Am.*, 116, 211–248, 1968.
- Druitt, T. H., and R. S. J. Sparks. On the formation of calderas during ignimbrite eruptions, *Nature*, 310, 679–681, 1984.
- Ferrara, G., and M. Treuil. Petrological implications of trace element and Sr isotope distributions in basalt-pantellerite series, *Bull. Volcanol.*, 38, 548–574, 1974.
- Garcia, S. R., W. K. Hensley, M. M. Minor, M. M. Denton, and M. A. Fuka. An automated multidecator system for instrumental neutron activation analysis of geological and environmental materials, in *Atomic and Nuclear Methods in Fossil Energy Research*, edited by R. H. Filby, B. S. Carpenter, and R. C. Ragains, pp. 133–140, Plenum, New York, 1982.
- Gardner, J. N., F. Goff, S. Garcia, and R. C. Hagan. Stratigraphic relations and lithologic variations in the Jemez volcanic field, New Mexico, *J. Geophys. Res.*, 91, 1763–1778, 1986.
- Goff, F., G. H. Heiken, S. J. Janyu, J. Gardner, S. Sell, R. Drake, and M. Shaltqullah. Location of Toledo caldera and formation of the Toledo embayment, Jemez Mountains, New Mexico, *Eos Trans. AGU*, 65, 1145, 1984.
- Govindaraju, K. 1984 compilation of working values and sample descriptions for 170 international reference samples of mainly silicate rocks and minerals, *Geostand. Newsl.*, 8, 3–16, 1984.
- Griggs, R. L. Geology and groundwater resources of the Los Alamos area, New Mexico, *U.S. Geol. Surv. Water Supply Pap.*, 1753, 1–107, 1964.
- Gromet, L. P., and L. T. Silver. Rare earth element distributions among minerals in a granodiorite and their petrogenetic implications, *Geochim. Cosmochim. Acta*, 47, 925–939, 1983.
- Halliday, A. N., A. E. Fallick, J. Hutchinson, and W. Hildreth. A Rb, Sr, and O isotopic investigation into the causes of chemical and

- isotopic zonation in the Bishop Tuff, California. *Earth Planet. Sci. Lett.*, **65**, 379-391, 1984.
- Harrison, T. M., and E. B. Watson. Kinetics of zircon dissolution and zirconium diffusion in granitic melts of variable water content. *Contrib. Mineral. Petrol.*, **84**, 66-72, 1983.
- Heiken, G., F. Goff, J. Stix, S. Tamanyu, M. Shafiqullah, S. Garcia, and R. Hagan. Intracaldera volcanic activity, Toledo caldera and embayment, Jemez Mountains, New Mexico. *J. Geophys. Res.*, **91**, 1799-1815, 1986.
- Hildreth, W. The Bishop Tuff: Evidence for the origin of compositional zonation in silicic magma chambers. *Spec. Pap. Geol. Soc. Am.*, **180**, 43-75, 1979.
- Hildreth, W. Gradients in silicic magma chambers: Implications for lithospheric magmatism. *J. Geophys. Res.*, **80**, 10,153-10,192, 1981.
- Hofmann, A. W. Diffusion in natural silicic melts: A critical review. In *Physics of Magmatic Processes*, edited by R. B. Hargrave. pp. 385-417. Princeton University Press, Princeton, N. J., 1980.
- Huppert, H. E., and R. S. J. Sparks. Double-diffusive convection due to crystallization in magmas. *Annu. Rev. Earth Planet. Sci.*, **12**, 11-37, 1984.
- Irvine, T. N. Heat transfer during solidification of layered intrusions. I. Sheets and sills. *Can. J. Earth Sci.*, **7**, 1031-1061, 1970.
- Izett, G. A., J. D. Obradovich, C. W. Haeser, and G. T. Crbula. Potassium-argon and fission-track zircon ages of Cerro Toledo Rhyolite tephra in the Jemez Mountains, New Mexico. *U.S. Geol. Surv. Prof. Pap.*, **1199-D**, 37-43, 1981.
- Jambon, A. Tracer diffusion in granitic melts: Experimental results for Na, K, Rb, Ca, Sr, Ba, Ce, Eu to 1300°C and a model of calculation. *J. Geophys. Res.*, **87**, 10,797-10,810, 1982.
- Kuentz, D. C. The Otowi Member of the Bandelier Tuff: A study of the petrology, petrography, and geochemistry of an explosive silicic eruption, Jemez Mountains, New Mexico. M.S. thesis, 165 pp., Univ. of Tex. at Arlington, Arlington, 1984.
- Kuentz, D. C., J. A. Wolff, S. D. Balsley, J. N. Gardner, P. R. Kyle, and S. Self. Compositional variation within the Lower Bandelier Tuff, Jemez Mountains, New Mexico. *Eos Trans. AGU*, **66**, 1143, 1985.
- Leaher, C. E. Effects of silicate liquid composition on mineral-liquid partitioning from Soret diffusion studies. *J. Geophys. Res.*, **91**, 6123-6141, 1986.
- Loeffler, B. M. Major- and trace-element and strontium- and oxygen-isotope geochemistry of the Polvaderra Group, Jemez volcanic field, New Mexico: Implications for the petrogenesis of the Polvaderra Group. Ph.D. thesis, 259 pp., Univ. of Colo., Boulder, Feb. 1984.
- Mahood, G. A. Chemical evolution of a Pleistocene rhyolitic center, Sierra La Primavera, Jalisco, Mexico. *Contrib. Mineral. Petrol.*, **77**, 129-149, 1981.
- Mahood, G. A., and W. Hildreth. Large partition coefficients for trace elements in high-silica rhyolites. *Geochim. Cosmochim. Acta*, **47**, 11-30, 1983.
- McBirney, A. R., B. H. Baker, and R. H. Nilson. Liquid fractionation. I. Basic principles and experimental simulations. *J. Volcanol. Geotherm. Res.*, **24**, 1-24, 1985.
- Müller, C. F., and D. W. Mittlefehdt. Depletion of light rare-earth elements in felsic magmas. *Geology*, **10**, 129-133, 1982.
- Müller, C. F., and D. W. Mittlefehdt. Extreme fractionation in felsic magma chambers: A product of liquid-state diffusion or fractional crystallization? *Earth Planet. Sci. Lett.*, **68**, 151-158, 1984.
- Minor, M. M., W. K. Hensley, M. M. Denton, and S. R. Garcia. An automated activation analysis system. *J. Radioanal. Chem.*, **70**, 459-471, 1982.
- Mittlefehdt, D. W., and C. F. Müller. Geochemistry of the Sweetwater Wash pluton, California: Implications for "anomalous" trace element behavior during differentiation of felsic magmas. *Geochim. Cosmochim. Acta*, **47**, 109-124, 1983.
- Murase, T. Viscosity and related properties of volcanic rocks at 800° to 1400°C. *J. Fac. Sci. Hokkaido Univ., Ser. F11*, **7**, 487-584, 1962.
- Nash, W. P., and H. R. Crocraft. Partition coefficients for trace elements in silicic magmas. *Geochim. Cosmochim. Acta*, **49**, 2309-2322, 1985.
- Newhall, C. G., and W. G. Melson. Explosive activity associated with the growth of volcanic domes. *J. Volcanol. Geotherm. Res.*, **17**, 111-131, 1983.
- Nielson, D. L., and J. B. Hulen. Internal growth and evolution of the Redondo dome, Valles caldera, New Mexico. *J. Geophys. Res.*, **89**, 8695-8711, 1984.
- Noble, D. C., and C. E. Hedge. Sr⁸⁷/Sr⁸⁶ variations within individual ash-flow sheets. *U.S. Geol. Surv. Prof. Pap.*, **650-C**, 133-139, 1969.
- Norrish, K., and B. W. Chappell. X-ray fluorescence spectrometry. In *Physical Methods in Determinative Mineralogy*, 2nd ed., edited by J. Zussman, pp. 201-272. Academic, Orlando, Fla., 1977.
- Pearce, J. A., and M. J. Norry. Petrogenetic implications of Ti, Zr, Y, and Nb variations in volcanic rocks. *Contrib. Mineral. Petrol.*, **69**, 33-47, 1979.
- Ponader, C. W., and G. A. Mahood. Soret diffusion in simple peralkaline silicate liquids near magmatic temperatures and pressures. *Geol. Soc. Am. Abstr. Programs*, **16**, 625, 1984.
- Rapp, R. P., and E. B. Watson. Monazite solubility and dissolution kinetics: Implications for the thorium and light rare earth chemistry of felsic magmas. *Contrib. Mineral. Petrol.*, **64**, 304-316, 1986.
- Rapp, R. P., F. J. Ryerson, and C. F. Miller. Monazite and allanite in the crust: Relevance to the distribution of the LREEs, Y, U, and Th. *Eos Trans. AGU*, **67**, 384, 1986.
- Schott, J. Thermal diffusion and magmatic differentiation: A new look at an old problem. *Bull. Mineral.*, **106**, 247-262, 1983.
- Self, S., F. Goff, J. N. Gardner, J. V. Wright, and W. M. Kite. Explosive rhyolite volcanism in the Jemez Mountains: Vent locations, caldera development and relation to regional structure. *J. Geophys. Res.*, **91**, 1779-1798, 1986.
- Shannon, R. D. Revised effective ionic radii and systematic studies of interatomic distances in halides and chalcogenides. *Acta Crystall.*, **5**, 1771-1776, 1976.
- Smith, R. L. Ash-flow magmatism. *Spec. Pap. Geol. Soc. Am.*, **180**, 5-27, 1979.
- Smith, R. L., and R. A. Bailey. The Bandelier Tuff: A study of ash-flow eruption cycles from zoned magma chambers. *Bull. Volcanol.*, **29**, 83-103, 1966.
- Smith, R. L., and R. A. Bailey. Resurgent cauldrons. *Mem. Geol. Soc. Am.*, **116**, 613-662, 1968.
- Smith, R. L., R. A. Bailey, and C. S. Ross. Geologic map of the Jemez Mountains, New Mexico, scale 1:125,000. *Geol. Invest. Map I-571*, U.S. Geol. Surv., Reston, Va., 1970.
- Sparks, R. S. J., H. E. Huppert, and J. S. Turner. The fluid dynamics of cooling magma chambers. *Philos. Trans. R. Soc. London, Ser. A*, **370**, 51-531, 1984.
- Turner, J. S., and I. H. Campbell. Convection and mixing in magma chambers. *Earth Sci. Rev.*, **23**, 255-352, 1986.
- Valentine, G. Procedures for analysis of silicate rocks and minerals at Los Alamos National Laboratory by X-ray fluorescence. *Los Alamos Natl. Lab. Rep.*, **L4-9663-MS**, 33 pp., 1983.
- Watshaw, C. M., and R. L. Smith. Ferromagnesian silicates in the Bandelier Tuff. *Geol. Soc. Am. Abstr. Programs*, **12**, 545, 1980.
- Watson, E. B. Apatite saturation in basic to intermediate magmas. *Geophys. Res. Lett.*, **6**, 937-940, 1979.
- Watson, E. B., and C. J. Capobianco. Phosphorus and the rare earth elements in felsic magmas: An assessment of the role of apatite. *Geochim. Cosmochim. Acta*, **45**, 2349-2358, 1981.
- Watson, E. B., and T. H. Green. Apatite/liquid partition coefficients for the rare earth elements and strontium. *Earth Planet. Sci. Lett.*, **56**, 405-421, 1981.
- Watson, E. B., and T. M. Harrison. Zircon saturation revisited: Temperature and composition effects in a variety of crustal magma types. *Earth Planet. Sci. Lett.*, **64**, 295-304, 1983.
- Watson, E. B., and T. M. Harrison. Accessory minerals and the geochemical evolution of crustal magmatic systems: A summary and prospectus of experimental approaches. *Phys. Earth Planet. Inter.*, **35**, 19-30, 1984.
- S. R. Garcia, INC-5, MS G776, Los Alamos National Laboratory, Los Alamos, NM 87545.
- F. Goff and G. Heiken, ESS-1, MS D462, Los Alamos National Laboratory, Los Alamos, NM 87545.
- M. P. Gorton and J. Stix, Department of Geology, University of Toronto, Toronto, Canada M5S 1A1.

(Received March 20, 1987;
revised August 31, 1987;
accepted September 22, 1987.)